April 2022

Stability Analysis of Delay-Driven Coupled Cantilevers Using the Lambert W-Function

Daniel Siebel-Cortopassi
University of South Florida

Follow this and additional works at: https://digitalcommons.usf.edu/etd

Part of the Applied Mathematics Commons, Mathematics Commons, and the Nanoscience and Nanotechnology Commons

Stability Analysis of Delay-Driven Coupled Cantilevers Using the Lambert W-Function

by

Daniel Siebel-Cortopassi

A thesis submitted in partial fulfillment
of the requirements for the degree of
Master of Arts in Mathematics
Department of Mathematics and Statistics
College of Arts and Sciences
University of South Florida

Major Professor: Sherwin Kouchekian, Ph.D.
Ivan Rothstein, Ph.D.
Boris Shekhtman, Ph.D.
Joel Rosenfeld, Ph.D.

Date of Approval:
June 16, 2022

Keywords: Delay differential equations, Microcantilevers, Stable regions, Coupled harmonic oscillators,
Decentralized control

Acknowledgments

I would like to thank my advisor Dr. Kouchekian for his insight, knowledge, and guidance, without which this paper would not have been written.

I would also like to thank all my professors I have had over the course of my studies here, especially Dr. Nagle, whose classes I absolutely enjoyed being in, and Dr. Curtin, whose classes introduced me to the basic graduate student workload. And of course, Dr. Kouchekian in his classes, which I very much enjoyed being in as well.

Thank you to all my friends in the department including Nathan, Zachary, Hunter, Himanshu, Boy-oon, Eion, and Paul for making my schooling so much more fun and enjoyable.

Table of Contents

List of Figures

Abstract

A coupled delay-feedback system of two cantilevers can yield greater sensitivity than that of a single cantilever system, with potential applications in atomic force microscopy. The Lambert W-function analysis concept for delay differential equations is used to more accurately model the behavior of specific configurations of these cantilever systems. We also use this analysis concept to find parameters which yield stability for greater parameter ranges, of the delay differential equations. The *Q factor*, or *quality factor*, is the ratio of energy stored in the system, to the energy lost per fixed oscillation/movement cycle. Having stability of the cantilevers corresponds to the physical system having a better Q factor and better sensitivity.

Chapter 1

Introduction

Simple harmonic motion, which is the simplest form of periodic motion, and its spinoffs are found everywhere in both mathematics and physics. Examples of simple harmonic motion are found in idealized spring-mass systems, pendulums and even in the process of hearing sound as the vibration of the eardrum. If a simple harmonic system were to be perfectly isolated from all outside forces and furthermore experiences no internal energy losses, then the system would continue its regular motion indefinitely. However, in any non-idealized environment it is true that there is some internal friction or energy losses in the system over time and such energy losses eventually dampen the motion by a non-trivial amount. The motion is also rarely, if ever, perfectly simple harmonic even if friction and internal losses are not part of the model. However, in many situations a system that is close enough to moving in simple harmonic motion can have a useful simple harmonic approximation. If one seeks to express systems of simple harmonic motion mathematically, this is generally done via expressing the plant as either a second order ordinary differential equation, or for multiple interacting moving bodies as a system of second-order ordinary differential equations. Damping and internal losses can be included in these mathematical equations for greater accuracy to the real world systems being described. There has been centuries of work in the fields of mathematics and physics done regarding the basic universal phenomenon of simple harmonic motion.

Simple harmonic motion is one-dimensional back and forth movement that, with some initial disturbance, initial velocity, or both, experiences acceleration along the one dimensional axis of movement. In any simple harmonic motion, the acceleration is proportional to the distance of the mass particle, or point mass, from some equilibrium position that is located somewhere on the axis of movement. Such motion is idealized as being the motion of a massless spring attached to some object mass, which is perfectly concentrated into a point. If such a mass object is at rest with the spring in its equilibrium position, then the system will not move as described by Newton's law of inertia. Once a force or an initial displacement, or both, is

applied to the system, the mass will begin to oscillate about the equilibrium point, and if there is no friction acting on the mass and no internal losses in the spring, this oscillation will continue indefinitely without losing amplitude. Although this is a significant oversimplification, examples of simple harmonic motion lie at the foundation of nearly all periodic movement in the real world. The simple harmonic oscillator model is also referred to, and will be referred to in this paper as, the spring-mass model.

Our discussion of the spring-mass model and so on will follow the format of the introductory material found in [22]. Motion that is simple harmonic can be described by any single sine or cosine function of time

$$X(t) = A \, sin(2\pi Bt), \tag{1.1}$$

and this equation describes a particle that oscillates with period $\frac{1}{B}$. With this system having no damping, friction, or internal losses, the periods are all identical to each other in every way, except for the time value increasing more with each consecutive period. By Hooke's law and Netwon's second law of motion, the general form of the equation of perfect simple harmonic motion is

$$m\frac{d^2 X}{dt^2} + kX = 0, \tag{1.2}$$

where m is the mass of the simple harmonic oscillator, and k is called the spring constant, with larger k meaning that the spring is stiffer. The SI unit of stiffness is N/m ; i.e., Newtons per meter. If we denote $\sqrt{\frac{k}{m}}$ by ω_0 , eq. (1.2) becomes

$$\frac{d^2 X}{dt^2} + \omega_0{}^2 X = 0, \tag{1.3}$$

which has general solution

$$X(t) = K_1 \, cos(\omega_0 t) + K_2 \, sin(\omega_0 t). \tag{1.4}$$

Note that the amplitude of oscillation is $\sqrt{K_1{}^2 + K_2{}^2}$. The *natural frequency* of the simple oscillator, commonly denoted by f_0 , is given by $f_0 = \frac{1}{2\pi}\sqrt{\frac{k}{m}}$. The natural frequency f_0 describes the number of cycles per unit time for the situation when the simple harmonic oscillator is not driven by any additional

time-dependent forcing function and has no damping. Another equivalent form of the solution to (1.3) is

$$X = K\,cos(\omega_0 t + \phi), \tag{1.5}$$

with K being the amplitude of oscillation and ϕ representing the initial phase of the harmonic motion. The velocity and acceleration of the particle both have the same form as the preceding equation and are immediately obtained via differentiation with respect to t as:

$$v(t) = \frac{dX}{dt} = -\omega_0 K\,sin(\omega_0 t + \phi), \tag{1.6}$$

$$a(t) = \frac{d^2 X}{dt^2} = -{\omega_0}^2 K\,cos(\omega_0 t + \phi). \tag{1.7}$$

Instead of as in these two forms (1.4) and (1.5), one can express the equations of simple harmonic motion in terms of initial displacement X_0 and initial velocity v_0. Utilizing the initial conditions, one finds:

$$K = \sqrt{{X_0}^2 + (\frac{v_0}{\omega_0})^2} \tag{1.8}$$

$$\phi = tan^{-1}(\frac{-v_0}{\omega_0 X_0})\,, \tag{1.9}$$

where $X_0 = K_1$ and $v_0 = K_2 \omega_0$.

When the harmonic motion of a particle is described by a linear combination of motion caused by two or more harmonic excitations, the displacement of the mass at time t is the sum of the displacement caused by each of the harmonic excitations taken separately. This phenomenon is known as the *principle of superposition*, and as long as the system is linear, which happens in many cases, this greatly simplifies working with harmonic oscillators in general. A system is linear if any vibration of the system does not influence the way the system responds to any other of the vibrations.

1.1 Damped Harmonic Oscillator

Damping is a force which can include, for example, dynamic friction, drag, and internal losses, that slows down over time the movement of individual components of a system such as the individual

components of a harmonic oscillator system. Throughout this paper, we will refer to the symbol γ as representing the entire effective damping force on the point mass. This total damping force adds another term to the simple harmonic oscillator equation, so the equation becomes

$$m\frac{d}{dt^2}X(t) + \gamma\frac{d}{dt}X(t) + kX(t) = 0 \tag{1.10}$$

or equivalently,

$$\frac{d}{dt^2}X(t) + 2\alpha\frac{d}{dt}X(t) + \omega_0{}^2 X(t) = 0, \tag{1.11}$$

where $\alpha = \frac{\gamma}{2m}$ and $\omega_0{}^2 = \frac{k}{m}$.

For the damped oscillator system, it is better to instead of considering Eq. (1.5), look at the complex version of the equation, i.e. to express the amplitude K and phase ϕ as a complex number via Euler's formula $e^{\pm i\theta} = cos(\theta) \pm i\,sin(\theta)$. Having $cos(\omega_0 t) = \Re(e^{\pm i\omega_0 t})$, substituting into (1.5) gives the defining equation

$$X(t) = \Re(Ke^{i(\omega_0 t + \phi)}) = \Re(Ke^{i\phi}e^{i\omega_0 t}) = \Re(\tilde{K}e^{i\omega_0 t}), \tag{1.12}$$

with $\tilde{K}$ being the *complex* amplitude, which is in other words the complex displacement at time $t = 0$. The *complex* displacement for arbitrary time t is $\tilde{X} = \tilde{K}e^{i\omega_0 t}$. A very quick calculation determines the complex velocity and acceleration to be

$$\tilde{v} = i\omega_0\tilde{X}, \tag{1.13}$$

$$\tilde{a} = -\omega_0{}^2\tilde{X}. \tag{1.14}$$

With this in mind, we can assume the solution is of the form $\tilde{X} = \tilde{K}e^{\lambda t}$ and make this common substitution into (1.11), resulting in

$$(\lambda^2 + 2\alpha\lambda + \omega_0{}^2)\tilde{K}e^{\lambda t} = 0, \tag{1.15}$$

which makes shown that it is needed to have either $\lambda^2 + 2\alpha\lambda + \omega_0{}^2 = 0$ or

$$\lambda = -\alpha \pm \sqrt{\alpha^2 - \omega_0{}^2} = -\alpha \pm i\sqrt{\omega_0{}^2 - \alpha^2} \tag{1.16}$$

and we let $\omega_d = \sqrt{\alpha^2 - \omega_0{}^2}$, which is the natural frequency of the *damped* oscillator. The natural frequency under damping is always less than what it is without damping (the oscillatory period is always slower in the damped case). Note that ω_d is an angular frequency.

The resulting solution of the equation is somewhat of a superposition of two $\tilde{K}$ terms, using the two different λ values, one for each of the two $\tilde{K}$ terms:

$$\tilde{X} = e^{-\alpha t}(\tilde{K}_{1_1}e^{i\omega_d t} + \tilde{K}_{2_2}e^{-i\omega_d t}). \tag{1.17}$$

The real portion of $\tilde{X}$ can, as in the undamped case, be written in a variety of ways such as

$$X(t) = e^{-\alpha t}(K_1 \cos(\omega_d t) + K_2 \sin(\omega_d t)), \tag{1.18}$$

with K_1, K_2 being constants as in the undamped version. If we take $t = 0$ in (1.18) and also its corresponding velocity v and acceleration a, we obtain the displacement in terms of X_0 and v_0 to be given by:

$$X(t) = e^{-\alpha t}(X_0 \cos(\omega_d t) + \frac{v_0 + \alpha X_0}{\omega_d} \sin(\omega_d t)). \tag{1.19}$$

The amplitude of the oscillations is given by $X_0 e^{-\alpha t}$. The motion in the damped case is not strictly periodic, but the time difference between each occurrence of the mass arriving at equilibrium from the same direction is always equal, and is $\frac{2\pi}{\omega_d}$. If $\alpha = \omega_0$ the system is *critically damped* and returns to equilibrium as quickly as possible without overshooting the equilibrium position. If $\alpha > \omega_0$, the mass will return to rest without oscillating, but will not return to the rest position as quickly as in the critically damped case. When the system is critically damped, the position of the mass is given by

$$X(t) = X_0(1 + \alpha t)e^{-\alpha t}. \tag{1.20}$$

In any damped case, the rate of total energy of the system lost is the damping force $-\gamma \frac{d}{dt}X(t)$ multiplied by the velocity $\frac{d}{dt}X(t)$. Comparing the damping force to the spring force can yield valuable information and the canonical way of doing this is to calculate the quality, or Q factor, of the system as follows (larger Q

factors are desired):

$$Q = \frac{k}{\gamma \omega_0} = \frac{\omega_0}{2\alpha}. \tag{1.21}$$

Typical Q values for microcantilevers can be much higher than 10,000.

1.2 Damped Harmonic Oscillator With Forcing Term

When an external time-varying force $f(t)$ influences the harmonic oscillator, then equation (1.10) becomes

$$m\frac{d}{dt^2}X(t) + \gamma\frac{d}{dt}X(t) + kX(t) = f(t). \tag{1.22}$$

This equation is easiest to work with in the specific case that $f(t)$ is a sinusoidal driving force of the form $f(t) = F_A\,cos(\omega(t - t_0))$ for some initial time t_0. In this case, the solution to the equation has two components. They are called the transient term, which is the part that dies out over time, and the steady-state term, which has in general an influence on the motion of the oscillator which does not decrease with increasing time. The transient component of the solution includes two arbitrary constants. The steady-state component of the solution, meanwhile, depends only on F_A and ω. We start with obtaining the steady-state portion of the solution, via expressing the equation in its complex form, i.e.

$$m\frac{d}{dt^2}\tilde{X}(t) + \gamma\frac{d}{dt}\tilde{X}(t) + k\tilde{X}(t) = F_A e^{i\omega t}, \tag{1.23}$$

which is a function that is linear in X. Since we also have the right side of the equation being a harmonic function, with angular frequency ω, the steady-state portion of the left hand side equation should also be harmonic with frequency equal to the frequency of the right hand side. Substituting $\tilde{X} = \tilde{A}e^{i\omega t}$, gives

$$\tilde{A}e^{i\omega t}(-\omega^2 m + i\omega\gamma + k) = F_A e^{i\omega t}. \tag{1.24}$$

Consequently,

$$\tilde{X} = \frac{F_A e^{i\omega t}}{k - \omega^2 m + i\omega\gamma}. \tag{1.25}$$

6

Using the notations $\tilde{F}_A = F_A e^{i\omega t}$, $\omega_0{}^2 = \frac{k}{m}$, and $\alpha = \frac{\gamma}{2m}$ (see [22]), the complex velocity $\tilde{v}$ is found via differentiating $\tilde{X}$. As a result, we arrive at:

$$\tilde{v} = \frac{\frac{\tilde{F}_A \omega}{m}}{2\omega\alpha + i(\omega^2 - \omega_0{}^2)}.$$
(1.26)

The steady-state position is the real part of (1.25), thus

$$X(t) = \Re\left(\frac{\tilde{F}_A}{i\omega\tilde{Z}}\right) = \frac{F_A}{\omega Z} sin(\omega t + \phi)$$
(1.27)

with $\tilde{Z}$ defined as $\frac{\tilde{F}}{\tilde{v}}$.

If the damping constant γ is small, the influence of the transient part of the solution to the harmonic oscillator equation does not decay rapidly; it can persist for quite some time, therefore the transient part needs to be taken into consideration in most spring-mass models. One phenomenon that may occur depending on the form of $f(t)$ is when resonance of some part of the system, or alternatively of the entire system, occurs. This generally happens when the frequency of the driving force $f(t)$ is close to the natural frequency f_0 of the harmonic oscillator system in question. Under resonance, the amplitudes of the oscillations increase greatly. In some situations, this resonance is desired but in others it can be very destructive, and can lead to bridges collapsing, components of machines breaking, etc.

What is desired is to find a general solution of (1.22). Since the equation (1.22) is linear, its general solution is a superposition of the homogeneous version of the equation, i.e. (1.10), and a particular solution of (1.22). The second, particular solution is the steady-state solution. The whole solution is given by

$$X(t) = Ae^{-\alpha t} cos(\omega_d t + \phi) + \frac{F_A}{\omega Z} sin(\omega t + \theta)$$
(1.28)

for some θ and arbitrary constants A, ϕ. When the system has weak enough damping, we can replace ω_d with ω_0 in the preceding equation and still have accuracy in the resulting model.

1.3   Introduction of Delay

When delay is introduced into a system of damped or undamped simple harmonic motion, the model becomes more complicated and much harder to analyze. In the past twenty years, there have been many novel papers published regarding the analysis of systems of delay differential equations, see [20]. A topic of current and recent research is analyzing their stability under different equation models and different systems of equations modeling different real-life systems as varied as internal combustion engines, sensing microcantilevers in atomic force microscopy (AFM), and transmission of brain waves between neurons in human and animal brains. One of the most prominent uses of microcantilevers is in sensing applications such as AFM.

1.4   Harmonic Oscillator With Delay

To the best of the author's knowledge, [19] is the first paper published regarding the modeling of a tapping mode AFM microcantilever via a delay differential equation constructed from the spring mass model; i.e. as a harmonic oscillator with the forcing term being purely a delay term. In the works [19, 20] and in this work as well, the delayed feedback forcing term is exactly the unknown equation in question, but at a previous time. Note that in our work the forcing terms are the same as in these previous works, except they are switched between the two equations of the system to achieve a coupling effect between the two microcantilevers in our new setup. This type of delay feedback is easy to implement in a laboratory setting, requiring a minimal number of components and complexity to feed the signal back into the movement of the cantilever itself via piezo-electric bimorphs holding the cantilevers in an easily obtainable AFM head.

In [19], the equation used to describe the movement of the microcantilever is

$$m\frac{d}{dt^2}X(t) + \gamma\frac{d}{dt}X(t) + kX(t) = -kGX(t - \tau), \tag{1.29}$$

with G being dimensionless gain which is the expression used for the product of the following components:

- constant displacement of the piezoelectric bimorph in proportional response to a displacement signal

- proportionality factor relating voltage to displacement of the cantilever from its average position

- amplification due to the amplifying electronics in the system

- variable gain, which via electronics can be increased or decreased to desired level and therefore allows entire G to vary as desired

They look for solutions to (1.29) that are of the form $z^{\alpha_z} e^{i\omega t}$, allowing ω to be complex. They also search for conditions under which such a solution can exist. Via substitution into (1.29) we have the equation (which must necessarily be fulfilled)

$$\omega^2 - \frac{i\gamma\omega}{m} - \frac{k}{m}(1 + Ge^{-i\omega t}) = 0. \tag{1.30}$$

Using this equation, they show how to predict gain-delay combinations in which successful amplification will occur. The parameters in (1.30) needed in using the equation for analysis are determined via experimental testing of a microcantilever setup of the form described in the first pages of their paper. In [19] and [20], the authors of those papers are interested in amplification of only the first harmonic of the cantilevers's vibration, as the first harmonic is the most easily detectable vibration mode. They look for combinations of time delay and gain, i.e. combinations of τ and G, which allow there to be a solution to (1.30) of the form $\omega = \omega'_f + i\beta$, with ω'_f being a frequency that is close to the cantilever's fundamental resonance frequency. β is a damping term. It is desired for the amplitude of the vibrations of the cantilever to increase with time, i.e. to have a *negative* value of β. [19] experimentally confirms that amplification is observed for negative β. Those experiments also verify the increase in resonant frequency that was predicted by the model. There was up to a 20 percent discrepancy between the spring mass model frequencies they calculated and the experimentally measured frequencies. They summarize that the amount of the discrepancy increased as τ increased and as G decreased.

1.5 Beam Equation With Delay

A similar approach to the one in [19] was employed in [20]. Instead of using the harmonic oscillator model, they used the Euler-Bernoulli beam equation to consider the microcantilever as a fixed-free beam of

nonzero length. The paper expanded on [19] and went a step further, examining stable and unstable regions in the τ, G plane in greater detail.

In [20] are described the non-longitudinal vibrations of the microcantilever by the (now partial) differential equation

$$EI\frac{\partial^4 Z(x,t)}{\partial x^4} + \mu\frac{\partial^2 Z(x,t)}{\partial t^2} + R(x,t) = F(x,t), \tag{1.31}$$

where R and F are forces per unit length. Utilizing the Kelvin-Voight form (see [20]), the damping function $R(x,t)$ can be written as:

$$R(x,t) = kZ(x,t) + \gamma\frac{\partial Z(x,t)}{\partial t}, \tag{1.32}$$

where k is the (positive) spring constant and γ is the (positive) damping constant due to internal and external losses of the cantilever. Also, in [20], it is assumed that the system has the same form of delayed feedback as assumed in [19]:

$$F(x,t) = -k'GZ(x,t-\tau), \tag{1.33}$$

where k' denotes the effective spring constant and the gain value G is, in contrast to the previous paper, allowed to be positive or negative. The real-world reason for this is that the piezoelectric bimorph may, for given position input data, push the microcantilever in either the same direction or the opposite direction as the input. Note that the direction stays constant for any gain or time delay combination and is based on the characteristics of the piezoelectric bimorph in the experimental setup.

For the purpose of simplifying the usage of the beam based delay differential equation that is used [20], the authors of the paper assume that the delayed feedback signal represents the state of the whole cantilever along its entire length at a previous time. This is a simplification of a general case. If it was not required to have a realistic chance of being able to use the model for analysis, the authors of [20] would have instead taken into account the fact that the measured signal from the laser pointed at the cantilever is only influenced by the vertical deflection of the cantilever at the spot the laser illuminates, which has illuminated diameter much smaller than the length of the cantilever. Since solving a delay differential equation requires continuous knowledge of the state of the system from τ to 0 seconds in the past, they use undriven eigenmodes of the cantilever as the previous knowledge required for this purpose. Then they arrive

at the final form of the delay differential equation they use to model the lever (of length L):

$$\frac{EI}{L^4}\frac{\partial^4 Z(x,t)}{\partial x^4} + \mu\frac{\partial^2 Z(x,t)}{\partial t^2} + \gamma\frac{\partial Z(x,t)}{\partial t} + kZ(x,t) = -k'GZ(x,t-\tau) \tag{1.34}$$

under the initial condition that the prefunction, ϕ, is a linear combination of the undriven eigenmodes of the cantilever on the time interval $[-\tau, 0]$ for each $x \in [0, L]$. The standard fixed-free beam boundary conditions are assumed as well.

The next step in their process is separating (1.34) via assuming it has the form $Z(x,t) = X(x)T(t)$, obtaining separate equations for time dependence and position dependence (with separation constant κ):

$$X^{(4)}(x) - \frac{L^4\kappa}{EI}X(x) = 0 \tag{1.35}$$

$$\mu T''(t) + \gamma T'(t) + (\kappa + k)T(t) = -k'GT(t-\tau). \tag{1.36}$$

The former equation of the two is canonical and its solutions are written up in [20]. Turning their attention to the latter equation, they look at the undriven case to find the solution of the homogeneous version of (1.36), i.e., the solution under the condition that the right hand side is zero. This allows them to in the paper express the prefunction $\phi(x,t)$ explicitly as

$$\phi(x,t) = \sum_{n=1}^{N} A_n X_n(x) e^{-\frac{\gamma t}{2\mu}} \cos(\omega_n t + \theta_n), \tag{1.37}$$

in which $A_n \cos(\omega_n t + \theta_n)$ is the nth harmonic with amplitude $|A_n|$ and initial phase θ_n. The reader is referred to the paper, [20], for definition of the terms used and clarification. As stated in the paper, taking $N = 3$ is large enough for most real-world situations.

After we have this general solution for (1.36), which consists of an infinite number of iterated solution terms in $n = 1, 2, \ldots$, for each fixed n, we get a differential equation with a delay term:

$$\mu T_n''(t) + \gamma T_n'(t) + (\kappa_n + k)T_n(t) = -k'GT_n(t-\tau) \tag{1.38}$$

with $\kappa_n = \frac{\lambda_n{}^4 EI}{L^4}$ with λ_n being the positive, increasing with n, roots of the equation $1 + cos(\lambda_n)\,cosh(\lambda_n) = 0$. Seeking a solution to (1.38) is the next step in their process, and $h(t) = e^{\beta_n t}$ solves (1.38) iff. β_n satisfies

$$\beta_n^2 + \frac{\gamma}{\mu}\beta_n + \frac{1}{\mu}(\kappa_n + k) = -\frac{k'}{\mu}Ge^{-\beta_n \tau} \qquad (1.39)$$

The general solution of (1.38) is

$$T_n(t) = \sum_m p_{n,m}(t)e^{\beta_{n,m}t}, \qquad (1.40)$$

where $p_{n,m}(t)$ can be any polynomial of degree smaller than the multiplicity of the root solution $\beta_{n,m}$. For each fixed n there are usually multiple solution roots $\beta_{n,m}$, therefore the notation. At long last, the general solution to (1.34) and any standard beam boundary conditions is given by

$$Z(x,t) = \sum_n \sum_m X_n(x)p_{n,m}(t)e^{\beta_{n,m}t}, \qquad (1.41)$$

with each polynomial $p_{n,m}(t)$ being determined by the initial condition. It is in most cases impossible to get an explicit solution for $Z(x,t)$. It is mentioned briefly that there is another method which continues the solution piece by piece without involving the aforementioned series solution. The authors of [20] instead choose to function on determining areas in the τ, G- plane where amplification succeeds. The type of amplification desired is of the frequencies close to the ω_n . So we all want to find a β_n that has both the properties $\Re(\beta_n) > 0$ and $\Im(\beta_n) \approx \omega_n$, i.e. a solution to (1.39) with these properties. They let $\beta_n = \alpha_n + i(\omega_n + \epsilon_n)$ with ϵ_n much smaller than ω_n and arrive at

$$\begin{cases} ((\alpha_n + \frac{\gamma}{2\mu})^2 - \epsilon_n(\epsilon_n + 2\omega_n))e^{\alpha_n \tau} = -\frac{k'}{\mu}G\,cos((\omega_n + \epsilon_n)\tau) \\ 2(\alpha_n + \frac{\gamma}{2\mu})(\epsilon_n + \omega_n)e^{\alpha_n \tau} = \frac{k'}{\mu}G\,sin((\omega_n + \epsilon_n)\tau)\,. \end{cases} \qquad (1.42)$$

It is an immediate result of these conditions that τ is bounded to always be inside allowed bands in the τ, G-plane. There are an infinite number of these bands and all the bands can be enumerated with only the

12

positive integers. The paper gives the unique solution of (1.42), given that τ, G satisfy

$$\begin{cases} (2p + \frac{1}{2})\pi < (\omega_n + \epsilon_n)\tau < (2p+1)\pi, \, for \, G > 0 \\ (2p + \frac{3}{2})\pi < (\omega_n + \epsilon_n)\tau < (2p+1)\pi, \, for \, G < 0 \end{cases} \quad (1.43)$$

for some $p \in \mathbb{N}$, and given that

$$G(\epsilon_n) = \frac{2(\alpha_n + \frac{\gamma}{2\mu})(\epsilon_n + \omega_n)}{\frac{k'}{\mu} sin((\omega_n + \epsilon_n)\tau)} e^{\alpha_n \tau}, \quad (1.44)$$

with α_n given via the following equation, which is the unique solution to (1.42):

$$\begin{aligned} \alpha_n(\epsilon_n) = &-\frac{\gamma}{2\mu} - (\epsilon_n + \omega_n) \cot((\omega_n + \epsilon_n)\tau) \\ &+ [(\epsilon_n + \omega_n)^2 (\cot((\omega_n + \epsilon_n)\tau))^2 + \epsilon_n(\epsilon_n + 2\omega_n)]^{\frac{1}{2}}. \end{aligned} \quad (1.45)$$

The paper [20] also determines whether the beam equation used was able to more accurately model the cantilever behavior than the harmonic oscillator model from [19]. According to the data they succeeded in reducing the discrepancies between the model data and the actual experimental data in comparison to the discrepancies found in the previous paper on the subject. For $|G|$ small enough, with the single beam model there are bands in the τ, G-plane of values of τ outside of which amplification is predicted to fail. Especially for negative gain, the beam model predicted regions of amplification with much more accuracy than the corresponding spring mass model did in [19]. One note is that according to [20] there is a wide variety of allowed τ and G values if amplification is desired. The restrictions on both are minimal, so stable regions may be found in many different areas of the τ, G-plane instead of only being concentrated in a small subsection (at least for realistic values of G and τ). The general conclusion about how well each model mirrors the real-life cantilever systems was that the single point mass model was not restrictive enough to the solutions of the main equation, and the single beam model was too restrictive. Therefore after having papers [19, 20] available, it is desired to seek a model system that lies in between the restrictiveness of the two different methods examined in these two papers.

1.6 Self-Coupled Harmonic Oscillator Pair

The work [15] examines various gain-delay regions in the τ, G_1-plane for a retarded delay differential equation system, which is the same type of system as we are considering in this paper. A retarded delay differential equation is a DDE which does not contain any delayed terms of the highest derivative in the system. For example, if the highest order derivative in the DDE is of fifth order, then the highest derivative term which has delay in it must be of fourth order or less, otherwise it is not a retarded system. Note that the systems we examine in this paper are all retarded systems. The constants in [15] are very different in magnitude from the ones the other papers use, because their experimental plant is a large macroscale spring mass system, while the other aforementioned papers deal with microcantilevers. The system in [15] is in essence a coupled harmonic oscillator system, and takes the coupling as if the two spring mass oscillators were attached to each other via a spring, while also having each of the two spring masses being influenced by its own delayed feedback. This is in contrast to our original systems, which have both spring masses/both cantilevers completely independent to each other except for the delay forcing, in which the output state of one influences the other, and vice versa via the delayed feedback of the piezoelectric bimorph. In each of these two papers, the two connected mass objects are identical with respect to each other.

The main results of [15] are their graphs in the τ, G_1-plane of the zero curves and stable and unstable regions for various delay time and gain combinations. In their work, as in ours, we take the time delay of the two feedback loops to also be the same with respect to each other. When there are two interacting bodies in a coupled system, whether the coupled model is of two harmonic oscillators or two beams, there are two gain values G_1, G_2 that can equally vary. The commonly used way to plot stability graphs for this type of coupled system is to fix either G_1 or G_2, and plot the other against delay time τ. Then the process is repeated to make one graph in the gain-delay plane for some various fixed values of the gain which is not on the graph axis, as is done in [15] and this work. Throughout their work, the zero curves of the stability exponent values are graphed, and the LWF method is used on one point from each of the areas bounded by the zero curves to determine whether the corresponding region is stable or unstable. Also in [15] are a handful of contour plots for some stable regions in a similar way to the contour plots presented in this work.

Their findings are as follows [15]: Introducing very small delay into weakly coupled oscillators that would be stable under zero delay condition destabilizes the system. Moderate and some large delays can make the system stable, especially when the $|G_i|$ are small. Still, the stable regions shrink as the $|G_i|$ are increased. When the gains become large enough, the system becomes unstable for all delay time choices.

Introducing very small delay into moderately coupled oscillators that would be stable under zero time delay does not necessarily destabilize the system. Some gain choices stabilize the system for delay time in the range of $0 < \tau < 3P$, where P is the period of the free oscillators. Moderate coupling, for the majority of system parameters, has a stabilizing effect when delay is present.

Introducing any delay into strongly coupled oscillators that would be stable under zero delay causes instability for most τ and G_i values. The pockets of stability found under such conditions are very small and sparse.

Note that the coupling referred to in his paper is direct physical coupling and not the delay coupling, which is only each point mass acting on itself. [15] assumes a decentralized control scheme, as our system does, which is defined as the controlled time delay being the same for all of the cantilevers/components.

1.7 General Equations

The general equation of simple harmonic motion is:

$$m\frac{d}{dt^2}Z(t) + \gamma\frac{d}{dt}Z(t) + kZ(t) = 0, \tag{1.46}$$

or equivalently,

$$\frac{d}{dt^2}Z(t) + \frac{\gamma}{m}\frac{d}{dt}Z(t) + \frac{k}{m}Z(t) = 0, \tag{1.47}$$

where γ is the damping coefficient. γ acts on the oscillator to make any initial velocity decay over time and eventually cease to move if there are no additional forces disturbing the system. The spring constant k represents the strength of the internal push-back, which pushes a spring that is displaced away from its equilibrium position back towards equilibrium.

Another model that can be used to predict microcantilever behavior is the beam model. The beam model has general equation representation

$$\frac{EI}{L^4}\frac{\partial^4 Z(x,t)}{\partial x^4} + \mu\frac{\partial^2 Z(x,t)}{\partial t^2} + \gamma\frac{\partial Z(x,t)}{\partial t} + kZ(x,t) = 0 \qquad (1.48)$$

with E, L, I, μ, γ being (respectively) Young's modulus, length of the cantilever, area moment of inertia, the mass per unit length at position x, and the internal damping term. k is the same resistive term as in the simple harmonic model. Equivalently to (1.48), we have

$$\frac{\partial^4 Z(x,t)}{\partial x^4} + \frac{\mu L^4}{EI}\frac{\partial^2 Z(x,t)}{\partial t^2} + \frac{\gamma L^4}{EI}\frac{\partial Z(x,t)}{\partial t} + \frac{kL^4}{EI}Z(x,t) = 0. \qquad (1.49)$$

This is a partial differential equation instead of an ordinary differential equation. Analysis of stability using the beam model is therefore generally more complicated than analysis of the simple harmonic oscillator model. However, the fixed-free beam equation more accurately models a microcantilever's dynamics than the harmonic oscillator model does, as is shown in [20]. This is because the typical microcantilever is in fact a rectangular or triangular fixed-free beam and not an actual spring mass system.

1.8 Normalizing

1.8.1 General Normalizing Process

Normalizing, also known as scaling, is a process commonly used in numerical simulation and modeling which involves converting all variables in a given system to dimensionless variables. Normalizing has three purposes:

- Making the independent and dependent variables dimensionless

- Making the size of all variables near 1 in magnitude

- Reducing the number of independent parameters

([16] p. 17). Some or all of these three purposes may be desired for any given situation. Specifically, making all terms or variables be near unity in magnitude can help greatly with computer modeling of a system as it

tends to reduce the manifestation of precision errors and inaccuracies, which are both inherent in computer models.

The process of normalizing for many different equation types and the process in general are extensively covered in [16]. For the sake of completeness, we will include a brief explanation of the general normalizing process here. The first step is to come up with a new, dimensionless variable corresponding to each of the variables in the original equation(s). So if t is a variable, the first step involves replacing t with a new variable $\bar{t} = \frac{t-t_0}{t_c}$, where $\bar{t}$ is a dimensionless number because the numerator and denominator have the same units, for example "$kg \; m \; s^{-1}$". t_c is called a "scale" of t. t_0 is generally chosen to be zero but in some fields of study, such as statistics, t_0 is often chosen to be nonzero and is called a "reference value" of t. The main task of scaling each variable is usually finding suitable scale for the variable. Note that in order to have $0 < |\bar{t}| < 1$ we must have $t_c = \max |t - t_0|$. This variable range is often the most desirable range to have each variable be for minimizing computational/modeling precision errors or calculation errors. In most digitized equations, for computational ease of accuracy it is generally best to have all variables in the range between 10^{-1} to 10^1.

There are five steps in scaling an equation:

- Identifying independent and dependent variables

- Making all the variables dimensionless

- "Inserting" the dimensionless variables into the equation(s) that is/are being normalized

- Making each term dimensionless

- Finding appropriate scales

The most basic example of the normalizing process for a differential equation follows and is found in [16]: We want to scale the equation given by

$$Y'(x) = -AY(x); \qquad Y(0) = K, \tag{1.50}$$

with $Y(x)$ being unknown and A, K given.

- Step 1: There is one dependent variable (Y), and one independent variable (x)

- Step 2: Define a dimensionless variable $\bar{x}$ to replace x, by $\bar{x} = \frac{x}{x_c}$. Same for the dependent variable Y, we define $\bar{Y} = \frac{Y}{Y_c}$.

- Step 3: Replace x with $x_c\bar{x}$ and Y with $Y_c\bar{Y}$. The derivative w.r.t. $\bar{x}$ is (via Chain Rule)

$$\frac{dY}{dx} = \frac{d(Y_c\bar{Y})}{d\bar{x}}\frac{d\bar{x}}{dx} = Y_c\frac{d\bar{Y}}{d\bar{x}}\frac{1}{x_c} = \frac{Y_c}{x_c}\frac{d\bar{Y}}{d\bar{t}} \tag{1.51}$$

So the equation has been transformed to

$$\frac{Y_c}{x_c}\frac{d\bar{Y}}{d\bar{x}} = -AY_c\bar{Y}; \qquad Y_c\bar{Y}(0) = K. \tag{1.52}$$

- Step 4: To make all the terms dimensionless, either divide by the coefficient of the highest derivative term or divide by the coefficient of one of the other terms, resulting in

$$\frac{d\bar{Y}}{d\bar{x}} = -Ax_c\bar{Y}; \qquad \bar{Y}(0) = \frac{K}{Y_c} \tag{1.53}$$

- Step 5: The same system can have multiple different suitable scales, depending on the reason for doing the scaling process. One possible choice of scales is based on desiring the size of $\bar{Y}$ and the other terms (i.e. the derivatives) to be unity, or at least close to unity. If unity is desired, $x_c = \frac{1}{A}$ is a good choice. Another good choice is, for this system, to use the "half-life" of the exponential decay as x_c , i.e. to set $x_c = \frac{ln(2)}{A}$.

When we look at choosing Y_c , one good choice, but not the only good choice, is to set $Y_c = K$, which yields $\bar{Y}(0) = 1$.

So with taking (for example) $x_c = \frac{1}{A}$ and $Y_c = K$, the properly nondimensionalized model is

$$\frac{d\bar{Y}}{d\bar{x}} = -\bar{Y}; \qquad \bar{Y}(0) = 1. \tag{1.54}$$

The common notation when using this process is to then drop the bars and work with the *already normalized* variables, which in doing this example we would then focus on dealing with the equation

$$\frac{dY}{dx} = -Y; \qquad Y(0) = 1. \tag{1.55}$$

1.8.2 *Normalizing Our Oscillator and Beam Equations*

First, our two equations in each coupled system are symmetric, i.e. the two cantilevers and all parameters regarding their intrinsic properties are the same (because the cantilevers we are modeling are both identical). So we can normalize each of the equations that are in the corresponding pair using exactly the same characteristic values for each of the two equations in the coupled model. In regards to our harmonic oscillator equation, we set $\bar{t} = \frac{t}{t_c}$, and choose characteristic time value to be $t_c = \sqrt{\frac{m}{k}}$ and get:

$$\frac{d}{d\bar{t}^2} Z(t_c\bar{t}) + \frac{\gamma}{\sqrt{mk}} \frac{d}{d\bar{t}} Z(t_c\bar{t}) + Z(t_c\bar{t}) = 0 \tag{1.56}$$

as our normalized harmonic oscillator equation. For the beam equation, we set both $\bar{t} = \frac{t}{t_c}$ and $\bar{x} = \frac{x}{x_c}$. We choose as characteristic values $t_c = \sqrt{\mu}$, $x_c = \frac{\sqrt[4]{EI}}{L}$ and obtain the normalized equation (for any length L)

$$\frac{\partial^4 Z(x_c\bar{x}, t_c\bar{t})}{\partial \bar{x}^4} + \frac{\partial^2 Z(x_c\bar{x}, t_c\bar{t})}{\partial \bar{t}^2} + \frac{\gamma}{\sqrt{\mu}} \frac{\partial Z(x_c\bar{x}, t_c\bar{t})}{\partial \bar{t}} + kZ(x_c\bar{x}, t_c\bar{t}) = 0. \tag{1.57}$$

Note that the initial/boundary conditions under these normalizations are changed by the normalizing process.

1.9 Overview of Paper

This paper seeks to, using the [24] QPMR toolbox and a program based on [15]'s procedure but written by the authors to verify the zero curve boundaries, in order to map the regions of stability and instability for a small variety of normalized systems of differential equations that model some arrays of coupled microcantilevers. This is done via using the matrix Lambert *W*-function for guaranteed convergence. We expand on [19, 20]. [19] models a single microcantilever system as a harmonic oscillator with the delay giving feedback to the single cantilever. [20] analyzes a single microcantilever system with the feedback, as in the preceding paper, affecting the one cantilever itself. The cantilever is modeled by the beam equa-

tion in [20], instead of being represented as a simple harmonic oscillator. This paper examines the stable and unstable regions of two coupled cantilevers using a system of two coupled second order damped harmonic oscillators, and alternatively using a system of two coupled fourth order beam-equation based partial differential equations.

Chapter 2

Stability

2.1 Definition

Stability is the matter of whether or not small changes in the initial conditions of a system of equations will have at largest a correspondingly small effect on the system's behavior as the elapsed time increases without bound. Whenever the goal is to use a computer model to predict the future behavior of a system, or alternatively to check if simulation data matches experimental data, then stability of the system is a requirement. If a system is unstable, the future state of the system predicted by the corresponding model may have little to no correlation to how the system will behave in the real world, and so the model can be useless. Asymptotic stability is a stronger form of stability, and is achieved whenever small changes/disturbances in the initial conditions will have, in the limit, vanishingly small effect as time $t \to \infty$. If a system is neither stable nor asymptotically stable, the system is called unstable. A simple undriven harmonic oscillator is never asymptotically stable when there is no damping. On the other hand, such an oscillator is always stable when there is a damping term in the equation. When there is a forcing term, i.e., the oscillator is driven by some non-constant force, the situation becomes much more complex. The general forcing terms that we consider in this paper are delay terms. Stability of a mathematical model is a necessary condition required for predicting or explaining behavior with any such model.

2.2 Some Commonly Used Stability Analysis Methods for DDEs

2.2.1 Zero Delay Case

For the case of a system with zero delay, the Routh-Hurwitz stability criterion can be used to determine whether or not all roots of a polynomial are located in the half plane $\mathbb{C}^- = \{z \in \mathbb{C} : \Re(z) < 0\}$. It

is computed via finding the principal minors of a matrix derived from the characteristic polynomial of the system. However, this criterion cannot yield relative stability; it can only confirm or deny the existence of stability. Also, the Routh-Hurwitz method does not work with the introduction of any delay [21].

When delay is added to a system, whether the system in question is based on the harmonic oscillator model or the beam model, the characteristic equation changes in character to having infinitely many roots as opposed to just finitely many roots in the delay-free case. As stated in [6] there are various methods of determining stability properties for systems such as the ones investigated in our study. The systems considered in this work are each a retarded linear time-invariant delay system, which is defined as any system of the form

$$\dot{X}(t) = \sum_{k=0}^{K} A_k X(t - \tau_k) \tag{2.1}$$

which has initial condition $X_0 = \phi \in \mathbb{R}^n$, constant matrix $A_k \in \mathbb{R}^{n \mathbf{x} n}$, and positive real numbers $\tau_k \in \mathbb{R}^+$ fixed and ordered as $0 = \tau_0 < \tau_1 < \cdots < \tau_K$. Note that the system is retarded if there is no delay in the highest derivative term. The following methods of stability analysis pertain to any retarded linear delay differential equation of the form just stated, and are all discussed in [6].

For a system of the form

$$\dot{\mathbf{X}}(t) = \mathbf{X}(t - \tau), \tag{2.2}$$

the *transfer function* of the time-delay system is defined as

$$\frac{\dot{\mathbf{X}}(s)}{\mathbf{X}(s)} = e^{-s\tau}. \tag{2.3}$$

2.2.2 Nyquist Plots

A loop transfer function $L(s) = P(s)C(s)$ is a function expression describing the effect of a two-way system of functions that modify some input signal to produce a possibly different output signal. Closed-loop systems are defined as feedback control systems, while open-loop systems do not have any feedback influencing the state. Thus, a closed-loop transfer function describes the net output of a feedback loop on some input source/input signal. Similarly, an open-loop transfer function refers to a transfer function that does not involve any feedback.

Its frequency response results from plotting the complex number $L(i\omega)$, as a function of ω. The resulting curve is called a Nyquist curve. This curve plot can be used to predict the stability of a closed loop system via information about its open loop behavioral tendencies. In fact, the number of poles of the closed loop system that are in the right half of the complex plane, S, satisfies $S = M + N$. Here M is the net number (not gross number) of clockwise encirclements of a point near the origin of $\mathbb{C}$ and N is the number of poles, of the loop transfer function, that are in the right half of $\mathbb{C}$. For closed loop stability, $S = 0$ must hold. If S is nonzero, the system is unstable.

2.2.3 Satché's Method

Satché's method is a modification of the Nyquist locus method that was originated in order to reduce the complexity of the Nyquist plot method, which can be quite complex for time-delay systems. Satché introduced this technique for delay systems, which uses the inverse Nyquist locus and also hinges on the use of a dual Nyquist method. First, the characteristic equation $\Delta = 0$ of the system is separated into two parts and the following procedure is done:

- $\Delta = D_1(s) + D_2(s)e^{-s\tau}$

- So we have $e^{-s\tau} + \frac{D_1(s)}{D_2(s)} = 0$. Each of $e^{-s\tau}$, $-\frac{D_1(s)}{D_2(s)}$ may be plotted in separate plots.

- The boundary of stability $e^{-i\omega\tau}$ is a unit circle on the Satché graph, i.e. all possible unstable roots are located in this unit circle. In the case that $e^{-s\tau} + \frac{D_1(s)}{D_2(s)}$ has no poles in the right half of the complex plane, the system is stable or unstable as follows:

- If $-\frac{D_1(s)}{D_2(s)}$ either encircles $0 + 0i$ or passes through the previously mentioned unit circle, the system is unstable.

- If neither of the preceding happens, the system is stable.

- If there are poles of $e^{-s\tau} + \frac{D_1(s)}{D_2(s)}$ in the right half complex plane, then the number of poles can be found by using the Nyquist criterion on only $D_2(s)$.

- Add this number of poles to the number of encirclements $-\frac{D_1(s)}{D_2(s)}$ makes around $0 + 0i$.

2.2.4 Padé Approximant Method

In the cases we are considering, and usually in general, a linear time delay system will have an irrational transfer function. The most common approximation used to express this transfer function as a rational function is the first-order Padé approximation:

$$e^{-s\tau} \approx \frac{1 - \frac{s\tau}{2}}{1 + \frac{s\tau}{2}} \tag{2.4}$$

The Padé method converts or simplifies an infinite-dimensional quasipolynomial to a simple, rational, finite-dimensional polynomial. With the Padé approximation replacing the exponential term in the characteristic equation, simplification gives

$$\delta(s) = \tau s^2 + (2 - \tau(a_0 - a_1))s - 2(a_0 + a_1), \tag{2.5}$$

in which a_0, a_1 are polynomials taken from the characteristic equation $\Delta = a_0(s) + a_1(s)e^{-s\tau} + a_2(s)e^{-2s\tau} + \cdots = 0$, as in [15]. (2.5) has only two pairs of roots instead of an infinite number of roots. Therefore analysis of the Padé approximated system is much easier than that of the original system. However, since it is an approximation, inaccuracies tend to occur. Specifically, the Padé method can appear to give false stability for some systems that are unstable.

2.2.5 Mikhailov's Method

The term Mikhailov's method refers to two different formulations, one of which can determine stability of a retarded time delay system. The Mikhailov criterion is based on the Nyquist plotting method, and like the Nyquist method, is a graphical analysis method. Although Mikhailov's method cannot be used for generating stability boundaries, it can be used to find whether or not a system is stable for a given combination of gain and time delay. The criterion holds for characteristic functions $\Delta(s)$ that satisfy the following:

- $\Delta(s)$ has no purely imaginary roots

- $\Delta(s)$ satisfies for the complex conjugate $* : L^*(s) = L(s^*)$

- $\lim\limits_{s->\infty} \frac{\Delta(s)}{s^{-k}} = A \neq 0$, with A a constant and k some integer.

Starting with $\omega = 0$, as ω increases without bound, $L(i\omega)$ rotates by the amount $\hat{\theta} = (-k - 2N)\frac{\pi}{2}$, where N is the number of characteristic roots with positive real parts [3]. Therefore, a necessary and sufficient condition that the system is stable is that $N = 0$. In other words, the system is stable iff.

$$\hat{\theta} = -\frac{k\pi}{2}. \tag{2.6}$$

2.2.6   Chu's Phase-Angle Locus Method

Chu's phase-angle locus method [8] is a modification of Evan's root-locus method. This is another graphical method, and the needed resulting figures can be quite difficult to construct, especially if the transfer function is complex in any way. A way to reduce the complexity is to superpose the phase-angle loci of each of the zeros and each of the poles of $\frac{C(s)}{A(s)}$, with the characteristic quasipolynomial being written in the form

$$\frac{C(s)}{A(s)}e^{-s\tau} = -\frac{1}{G}, \tag{2.7}$$

G being a gain value. This method is briefly summarized in [6]; it is noted that computer plotting greatly simplifies the construction of more complex loci, but this method is still more time-consuming than other methods.

2.2.7   Direct Method (W-method)

This method is also summarized in [6] and that paper goes into a more detailed description and includes examples. The reader is referred to the corresponding paper and a brief summary of the method is included here. The W-method can be used for a single delay τ and can be extended to cover cases of multiple delays as well. The process briefly summarized is as follows:

- Determine the location of the characteristic roots for the zero delay case

- Consider $0 < \tau < \epsilon+$ and the infinitely many new roots' positions. Find the points where the loci cross or touch the vertical axis and the corresponding τ values.

- Find which of the values are stabilizing and which are destabilizing, which yields stable and unstable ranges of delay.

2.2.8 *Temporal Locus Method*

The first appendix of [6] includes a temporal locus method based on Euler-Newton continuation, and includes a detailed algorithm and MATLAB program. The details will not be repeated here, as it would take up a sizable amount of this paper. We do not employ this method in this paper, using instead the Lambert W-function method.

2.3   Definition of the Lambert *W*-Function

The Lambert W-function method for delay differential equations is a commonly used method of determining stability for a particular system of differential equations. The Lambert W-function, which we will denote in this paper as simply W (scalar case) or $\mathbf{W}$ (matrix case) is defined as the solution of the equation

$$W(z)e^{W(z)} = z \tag{2.8}$$

with the function $W : \mathbb{C} \to \mathbb{C}$. The matrix Lambert W-function is the main tool of the MATLAB program set we use in this paper.

Having similarities to the complex log function, W is in fact a multivalued function, i.e., there are infinitely many solutions to $W(z)e^{W(z)} = z$ for any complex z. Taking branch cuts and referring to them separately allows us to have $W_k(z)$ be a one-to-one invertible function for each branch, k. If z is restricted to the real numbers, there are only two k values for which $W_k(z)$ takes real values: the *principal branch* $k = 0$, and the branch corresponding to $k = -1$. A graph of these two branches and where they meet is shown in Fig (1).

The following definition of the matrix version of the Lambert W function, "$\mathbf{W}$", is taken directly from [7] and is canonical. Suppose $\mathbf{M}$ is an $n \times n$ matrix with complex-valued entries,
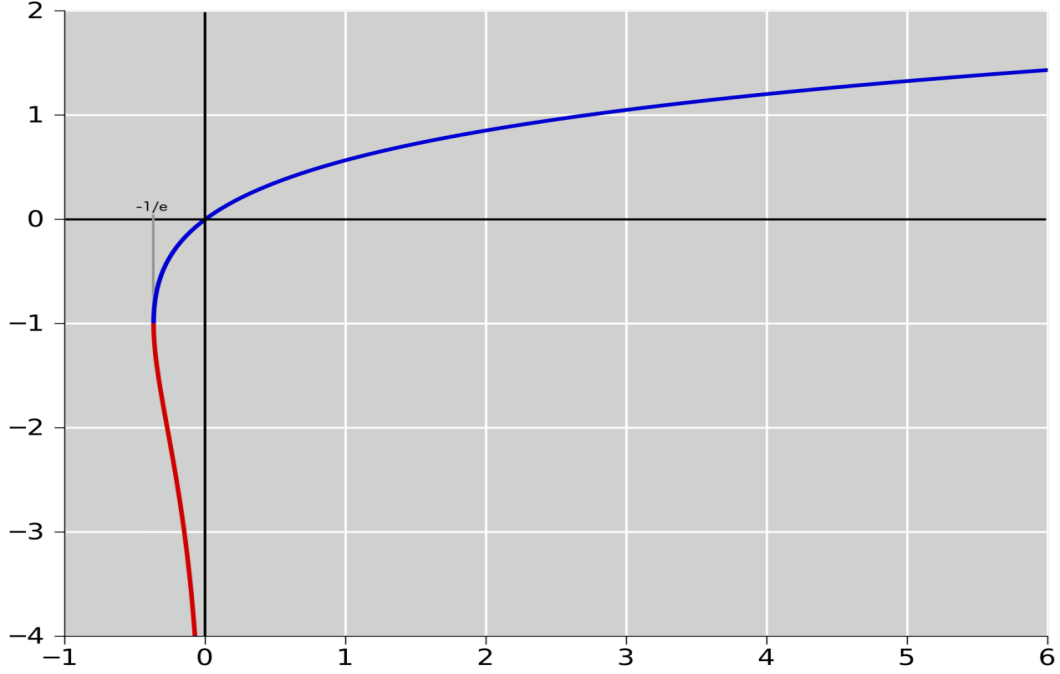
Figure 1.: Lambert W-function branches $k = 0$ (blue) and $k = -1$ (red). These are the only branches of the Lambert W function which take real values. Taken online from Wikimedia Commons search result for "Lambert W Function", public domain license.

with $\mathbf{HJH}^{-1}$ as its Jordan normal form where

$$
\mathbf{J} = \begin{bmatrix} \mathbf{J}_1(\lambda_1) & & \\ & \ddots & \\ & & \mathbf{J}_p(\lambda_p) \end{bmatrix}, \tag{2.9}
$$

and $\lambda_1, \ldots, \lambda_p$ are the eigenvalues of $\mathbf{M}$. For each branch k, define $\mathbf{W}_k$ of a Jordan block of size t as:

$$
\mathbf{W}_k(\mathbf{J}_i) = \begin{bmatrix} W_k(\lambda_i) & W_k^{'}(\lambda_i) & \cdots & \frac{1}{(t-1)!} W_k{}^{t-1}(\lambda_i) \\ 0 & W_k(\lambda_i) & \cdots & \frac{1}{(t-2)!} W_k{}^{t-2}(\lambda_i) \\ \vdots & \vdots & \cdots & \vdots \\ 0 & 0 & \cdots & W_k(\lambda_i) \end{bmatrix}, \tag{2.10}
$$

and set

$$\mathbf{W}_k(\mathbf{M}) = \mathbf{H} \begin{bmatrix} \mathbf{W}_k(\mathbf{J}_1\lambda_1) & & \\ & \ddots & \\ & & \mathbf{W}_k(\mathbf{J}_p\lambda_p) \end{bmatrix} \mathbf{H}^{-1}. \tag{2.11}$$

It follows that $\mathbf{W}_k(\mathbf{M})$ satisfies

$$\mathbf{W}_k(\mathbf{M})e^{\mathbf{W}_k(\mathbf{M})} = \mathbf{M}. \tag{2.12}$$

The matrix $\mathbf{W}_k(\mathbf{M})$ defined as in (2.12) is called the matrix version of the Lambert W-function for the branch k.

2.4 Determining Stability Via the Lambert W-Function

Using the Lambert W-function, denoted LWF, stability of individual points in the τ, G-plane can be determined. A mesh plot of these points can via MATLAB or any similar language yield a contour plot of stable and unstable regions with varying levels of stability.

The scalar delay differential equation case will be demonstrated first and then the use of the LWF in the case of systems of delay differential equations will be described briefly, as was done in [7]. A scalar homogeneous DDE is given by

$$\dot{Y}(x) = aY(x) + bY(x - \tau), \tag{2.13}$$

with τ being the time delay, which is always positive. The characteristic equation of this simplest DDE is $s - a - be^{-s\tau} = 0$. The solution to (2.13) can easily be expressed [2, 9, 34, 28] in terms of W and takes on the form

$$s_k = \frac{1}{\tau}W_k(\tau be^{-a\tau} + a), \tag{2.14}$$

with k indicating which branch of W is to be used. Each single root, out of the infinitely many roots of (2.13), has a correspondence to one of the branches k of W. Within all the solutions (2.14), the solution corresponding to the 0-th branch, which is the principal branch W_0, always has the largest real part in the scalar DDE case. This is not always true in higher order cases, and a second order counterexample is given in [7]. Out of all of the real parts of the (complex) eigenvalues of the matrix s_k, the largest such real part

is called the *stability exponent*. The stability of the whole system is completely determined by the sign of the stability exponent. If the stability exponent is negative, the system is stable. On the other hand, if the stability exponent is positive, the system is unstable. Note that the stability exponent is found via searching *all* branches $k = \pm[0, 1, 2, ...]$ for any particular DDE system. However, in most (but not all) practical cases, it suffices to take the branches $k = [-1, 0]$.

Purely numerical methods for finding the stability exponent, such as the Padé approximant method, can result in stable regions "spilling over" to unstable regions in a significant manner. This unwanted phenomenon is because whatever solver being used tends to, for some areas in the τ, G-plane, converge to another stable root instead of the stability exponent [15]. There is, as of this writing, no known way to guarantee that the root the solver converges to is in fact the stability exponent of the system, for purely numerical methods. The major strength of the Lambert W-based method is that it is the only currently known method for which convergence to the stability exponent is guaranteed.

Yi, Ulsoy, and Asl introduced the commonly used method of using the matrix LWF "**W**" to compute characteristic roots of the system for a higher order DDE model. When there is a higher order DDE of the form

$$\dot{\mathbf{Y}}(x) = \mathbf{A}\mathbf{Y}(x) + \mathbf{B}\mathbf{Y}(x - \tau), \tag{2.15}$$

with $\mathbf{Y} \in \Re^n$, $\mathbf{A}, \mathbf{B} \in \Re^{n \times n}$ and positive delay time τ, the method of finding stability for a particular system is based on obtaining a solution of

$$\mathbf{S} - \mathbf{A} - \mathbf{B}e^{-\mathbf{S}\tau} = \mathbf{0} \tag{2.16}$$

so we can then obtain the eigenvalues of $\mathbf{S}$. ($\mathbf{S} \in \mathbb{C}^{n \times n}$). $\mathbf{A}$ and $\mathbf{S}$ do not commute (since $\mathbf{A}$ and $\mathbf{B}$ do not commute). So we cannot solve for $\mathbf{S}$ in one go. One way around this is to use $\mathbf{W}$. From the characteristic equation of the original system, i.e.

$$\det\left(\mathbf{S} - \mathbf{A} - \mathbf{B}e^{-\mathbf{S}\tau}\right) = 0, \tag{2.17}$$

we have (rearranged and multiplied by $\tau e^{-\mathbf{A}\tau}$)

$$\tau(\mathbf{S} - \mathbf{A})e^{\mathbf{S}\tau}e^{-\mathbf{A}\tau} = -\mathbf{B}\tau e^{-\mathbf{A}\tau}. \tag{2.18}$$

In order to use the property of the Lambert W-function that $\mathbf{W}(t)e^{\mathbf{W}(t)} = t$ to solve (2.16), we introduce another, unknown matrix $\mathbf{Q}$ with the property that

$$\tau(\mathbf{S} - \mathbf{A})e^{\tau(\mathbf{S}-\mathbf{A})} = -\mathbf{B}\tau\mathbf{Q}. \tag{2.19}$$

Since $\mathbf{W}(\mathbf{K})e^{\mathbf{W}(\mathbf{K})} = \mathbf{K}$ for any matrix $\mathbf{K}$, we take the LWF of both sides of (2.19) and get

$$\mathbf{W}(\tau(\mathbf{S} - \mathbf{A})e^{\tau(\mathbf{S}-\mathbf{A})}) = \mathbf{W}(-\mathbf{B}\tau\mathbf{Q}), \tag{2.20}$$

i.e.

$$\tau(\mathbf{S} - \mathbf{A}) = \mathbf{W}(-\mathbf{B}\tau\mathbf{Q}). \tag{2.21}$$

Solving for $\mathbf{S}$, we get

$$\mathbf{S}_k = \frac{1}{\tau}\mathbf{W}_k(-\mathbf{B}\tau\mathbf{Q}_k) + \mathbf{A}, \tag{2.22}$$

for any k-th branch of $\mathbf{W}$. However, $\mathbf{Q}_k$ is still unknown. To solve for $\mathbf{Q}_k$ we substitute equation (2.22) into equation (2.18) which gives the following equation,

$$\mathbf{W}_k(-\mathbf{B}\tau\mathbf{Q}_k)e^{\mathbf{W}_k(-\mathbf{B}\tau\mathbf{Q}_k)+\mathbf{A}\tau} = -\mathbf{B}\tau, \tag{2.23}$$

which is a nonlinear equation that can be solved directly with any of the common mathematical language numerical solvers. This can be done either with or without an initial guess for the matrix $\mathbf{Q}_k$. For example, in MATLAB one can use "vpasolve", or alternatively use "fsolve" with an initial guess, for finding the entries of the $\mathbf{Q}_k$ matrix for some chosen k. The standard initial guess for using a solver similar to "fsolve" is $\mathbf{Q}_k = e^{-\mathbf{A}\tau}$. After computing $\mathbf{S}_k$, the candidates for the stability exponent are the real parts of each of the eigenvalues for all k.

Chapter 3

Delay Differential Equations

3.1   Notation and Basics

A Delay Differential Equation (*DDE*, *Delay DE*) is a differential equation that has the derivative with respect to time, depend on the solution of the DE at previous times. Such an equation may or may not also have the time derivative depend on the derivative of the solution at previous times. The general form of a delay differential equation is

$$\begin{cases} \mathbf{X}'(t) = \mathbf{A}\mathbf{X}(t) + \mathbf{B}(t - \tau), t \geq t_0 \\ \mathbf{X}(t) = \phi(t), t \leq t_0 , \end{cases} \tag{3.1}$$

with $\mathbf{A}, \mathbf{B}$ some real or complex coefficient matrices in $\mathbb{R}_n$ or $\mathbb{C}_n$, and $0 < \tau \in \mathbb{R}$. (The specific class of delay equations this paper investigates has $\mathbf{A}, \mathbf{B}$ as square 4 by 4, 2 by 2, 8 by 8, etc. matrices) A coupled 4th order delay system tends to have an 8 by 8 coefficient matrix in the above formulation. Simplification techniques can yield a sufficiently representative 4 by 4 matrix for the same system. We will discuss this in additional detail later in this paper. DDE systems may be expressed in alternate forms, such as

$$\begin{cases} \mathbf{X}'(t) = \mathbf{F}(t, X(t), X(t - \tau_1), \ldots, X(t - \tau_{k_1}), X'(t - s_1), \ldots, X'(t - s_{k_2})) \\ \mathbf{X}(t) = \phi(t), t \leq t_0. \end{cases} \tag{3.2}$$

If the right hand side of the preceding equation includes one or more terms depending on the derivative, then the equation is called a *neutral* delay differential equation. If no right hand side derivative terms appear, the equation is called a *retarded* delay differential equation. Alternatively, these equations can be denoted as Retarded/Neutral functional differential equations, or RFDEs/NDDEs for short.

The most general expression of a delay differential equation system is

$$\begin{cases} X'(t) = F(t, X_t), t \geq t_0 \\ X_{t_0} = X(t_0 + \theta) = \Phi(\theta), \end{cases} \tag{3.3}$$

with $X_t := X(t + \theta), \theta \in [-r, 0]$, being a function in the Banach space $C = C^0([-r, 0], R^d)$ of continuous functions mapping the interval $[-r, 0]$ into R^d, and F is a given function which maps the set $\Omega \subseteq R \times C$ into R^d (as stated in [4]). Note that instead of having a single-time initial condition as in an ordinary differential equation system, delay differential equation systems require some function defined on a continuum as the initial condition.

The delays may be constant, or functions of t i.e. $\theta = \theta(t)$. The time delays θ may even be a function of both t and $X(t)$. This latter case is referred to as the *state dependent* delay case.

Many real-world phenomena can be modeled and predicted by ordinary differential equations. However, ODEs do not take into account time delay in the system dynamics, which tends to exist in physical reality (at the most basic level, even light does not travel instantly). Delay differential equations, which include time delays in their defining equations, can therefore model and predict the behavior of these phenomena more accurately. However, there are many differences between DDEs and ODEs, and working with DDEs is more difficult than working with their ODE counterparts. Still, the field of delay differential equations has been an active area of research in the most recent decades. When delay terms are included in an equation model, they can often have significant effects on the behavior of the system. They can induce or increase either stability or instability and affect many of the other properties of the system, regardless of whether the corresponding ordinary differential equation system was originally stable or unstable.

The method of steps is the most often used method of solving more simple delay differential equations. If there is a single delay τ in the right hand side, the solution of the original DDE with initial condition continuum $\phi : [-\tau, 0] \to \mathbb{R}^n$ is found for the time interval $[0, \tau]$. The solution on this time interval is found by solving the initial value problem

$$\begin{cases} \frac{d}{dt}\psi(t) = F(\psi(t), \phi(t - \tau)) \\ \psi(0) = \phi(0) \end{cases} \tag{3.4}$$

for $\psi(t)$. $F(\psi(t), \phi(t - \tau))$ is taken from the original delay equation's right hand side, $F(X(t), X(t - \tau))$. This process is repeated for the succeeding interval of length τ, using the solution of the most recently found τ-interval of solution as the initial "condition"/state. This can theoretically be repeated indefinitely to find the solution on arbitrary interval sets [a] by finding the solution $\psi(t)$ on all of the τ-intervals containing some part of [a].

3.2 History of DDEs and Some DDE Methods

This section includes information from [1]. Differential equations belong to the class of functional differential equations, and this more general class of equations been studied for over two centuries. Their study was first initiated by those working in the fields of number theory and geometry. Past engineers and mathematicians had already known about the presence of delay effects on systems, but the theory enabling them to employ delayed systems was not developed until relatively recently. With the advent of early computers, real-world inspired models in the form of delay differential equations became much more useful and the theory saw an explosion in development. Once computers had started being incorporated into control systems everywhere, the theory of delay differential equations was then everywhere and began a period of massive development.

The majority of research regarding functional differential equations focused on linear equations. Specifically, most functional differential equation (FDE) research focused on either instability or the preservation of stability under small, nonlinear perturbations for which the linearization had been either unstable or stable [1]. The Laplace transform was always widely used in the specific case of when the equations are linear and have constant coefficients. The logical extension of using the Laplace transform on these systems is to expand solutions in terms of the eigenfunctions and focus on the convergence properties of these eigenfunction expansions. Existence and uniqueness results, parameter dependence, and continuation of solution results for FDE/DDE equation systems are very similar to the corresponding results for ordinary differential equations (ODEs). However, there are some differences, mainly due to the fact that delay differential equations are infinite-dimensional systems.

Beginning attempts at finding numerical solutions of delay differential equations were first undertaken in the 1950's, and these early attempts were focused on only systems with either constant or time-

dependent delays. They tended to use linear, multistep methods that had been developed for ODEs and modified to be used on DDEs. The specific class of equations most of these early works dealt with [4] was equations of the form

$$\begin{cases} \mathbf{X}'(t) = F(t, \mathbf{X}(t), \mathbf{X}(t - \tau(t))), & t_0 \leq t \leq t_f \\ \mathbf{X}(t) = \phi(t), & t \leq t_0. \end{cases} \quad (3.5)$$

These attempts often assumed that a specified type of mesh points existed, and then would use such a mesh with any arbitrary discrete method, the discrete method having the property of using nodal points only. In this situation, any such method could be applied directly to retarded or neutral delay equations. This requirement regarding existence and types of mesh points is an extremely severe restriction, and makes the aforementioned early methods unusable in many cases. It often happens that the solution is not smooth enough which makes extension of the direct method to higher order multistep formulas impossible. If this happens, one can employ a modified Taylor expansion formula which was initially conceived in [36],

$$\sum_{i=0}^{k} \alpha_i X_{n+i} = h \sum_{i=0}^{k} \beta_i F(t_{n+i}, X_{n+i}, X_{n+i-m}) + T(\delta_n), \quad n = 0, 1, \ldots, \quad (3.6)$$

to be the basis of another type of method. This is called the *modified method*. In (3.6) the correction terms $T(\delta_n)$ depend on the jumps δ_n in the derivatives of $\mathbf{X}(t)$ at the mesh points. The modified method is only used at the beginning of the integration, up until the solution is sufficiently smoothed out [4]. If the DDE is of the neutral type, then because smoothing does not occur in the neutral case, the modified method must be used for the entire integration interval. Feldstein and Cryer/Tavernini proposed selection of mesh points separately from delay, and theory for higher order methods, respectively. Cryer and Tavernini produced papers regarding both one step and multistep methods for Volterra functional differential equations [4], a more general class of equations.

Linear retarded DDEs, which are the focus of this paper, can be expressed in the form $f : C \to \mathbb{R}^n$ with f being a continuous linear functional. There is a solution to the linear retarded system, of the form $e^{st}c$ for some nontrivial n-component vector c iff. s satisfies the characteristic equation [1]

$$\det \Delta(s) = 0, \quad \Delta(s) = sI - f(e^{-s})I, \quad (3.7)$$

34

with I being the identity matrix. The (complex) numbers s satisfying this equation are its eigenvalues. There can be infinitely many solutions to the characteristic equation (3.7), but in any vertical strip of the complex plane there is only a finite number of these eigenvalues. If there is at least one eigenvalue of (3.7) that has a positive real part, then the system is unstable. All of the eigenvalues s have a negative real part if and only if the system is asymptotically stable. The most widely used stability analysis method for DDEs is to find the rightmost eigenvalue s. This is not easy, and a lot of theory has been developed to increase the efficiency of the process of finding this desired eigenvalue. Many improvements can likely still be made in this area.

In the nonlinear RFDE case, if the zero equilibrium has the property that all its eigenvalues have negative real parts, Gronwall-type inequalities and a variation of constants formula (classical approaches) can be used to prove that the zero equilibrium for the nonlinear equation is asymptotically stable. In the same way, if one or more of the eigenvalues of the zero equilibrium have positive real part then the system is unstable. However, for nonlinear RFDEs that have zero as an equilibrium and also the property that the zero solution of the (linear) variational equation is not asymptotically stable, but on the other hand has no eigenvalues with positive real part, then the classical methods do not give any useful information [1]. When this happens, it is possible to modify Lyapunov methods to be used with the RFDE being examined.

3.3 Example of a Typical Real-World DDE

The paper [20] examines the theory and setup of a delay-differential equation inspired by the Euler-Bernoulli beam equation. They use the E-B equation to model the behavior of a microcantilever that has its current position state depend explicitly on the position state of the cantilever at a previous time. In their system the forcing term is the only delay term in the equation. The real-world system corresponding to the model is (as an example) the cantilever in an atomic force microscope. The deflection of the cantilever is measured by a detector and then fed back into the piezo-electric bimorph that is holding the cantilever with variable time delay and variable gain controllable by the user, which results in additional forced movement of the microcantilever. The desired outcome is to be able to choose and predict gain-delay combinations that can increase the sensitivity accuracy of the microcantilever to changes in the surface being imaged, i.e., the Q-factor of the atomic force microscope. There are many other applications in which the same type of modeling via similar delay-differential equations can increase performance.

The main equation studied in [20] is a fourth-order partial differential equation with the delay feedback as the forcing term.

3.4   Differences Between ODEs and DDEs

There are many differences between ODEs and DDEs, and as previously stated, working with DDEs is generally more complicated than working with ODEs. Different methods are needed because DDE analysis is fundamentally different from the analysis of ODEs.

One difference is that although with ordinary DEs you can integrate backwards in time to find the history of the solution, when dealing with delay DEs this cannot be done in general. For example, the solution of a specific DDE can possibly be a constant value for all nonnegative time. However even if one has the complete nonnegative (in this case, constant) time solution of the DDE, the solution for the negative time interval continuum, i.e. the initial function (and anything happening "before" the initial function) cannot be uniquely determined unless given.

Propagation of discontinuities occurs in DDEs differently than in ODEs and often leads to imperfections in solving whatever DDE is at hand. This does not introduce as much difficulty in retarded DDEs, in which smoothing of discontinuities occurs with increasing time. However, this was originally an issue that had to be overcome when working with neutral DDEs. There is no smoothing of the solution when dealing with neutral DDEs, so the discontinuities are propagated indefinitely forward in time at every multiple of *each* of the delays present in the system.

One of the most fundamental differences between ODEs and DDEs is that of their initial conditions. With ordinary differential equations, the only initial condition needed is the result value at a single time. On the other hand, with delay differential equations the initial condition must be a function on a continuum, i.e. on an interval of time history instead of just one point. Another fundamental difference which makes DDEs much harder to analyze than ordinary DEs is that delay equations belong to the class of systems which are infinite dimensional, while their counterparts ordinary DEs belong to the class of systems which are finite-dimensional. Therefore, delay differential equations in complexity resemble ordinary differential equations less than they resemble partial differential equations, and this is a reason why DDEs are likewise harder to work with.

3.5   Existence and Regularity of Solutions

As is standard in the general field, we must at the beginning of the theory concern ourselves with existence of solutions on an interval, uniqueness of solutions, broadening such interval of existence when it does exist, and whether or not solutions have continuity based on the system-defining parameters such as the given solution on the pre-interval.

Existence, uniqueness, and regularity results for some specific classes of both neutral DDEs and more specified state dependent delay equations have been under development by many sources, especially in the most recent twenty years. However, the general theory of existence, uniqueness, and regularity of solutions for these classes of delay equations remains elusive. This is in contrast to DDEs with fixed delays, time dependent delays, and also retarded delay equations in general, which all have their basic theory well developed.

The various different types of delay often cause discontinuities in the solutions which can propagate in different ways. These discontinuities make it more difficult to design effective numerical methods for modeling DDEs. Also, the fact that delay systems may be coupled in many different ways is another factor that can affect how the discontinuities propagate. In the following discussion, τ, σ are the delay term(s) and the delay derivative term(s), respectively, in the right hand side of the DDE/NDDE

$$\begin{cases} \mathbf{X}'(t) = \mathbf{F}(t, \mathbf{X}(t - \tau), \mathbf{X}'(t - \sigma)), & t_0 \leq t \leq t_1 \\ \mathbf{X}(t) = \phi(t), & t \leq t_0 \end{cases} \tag{3.8}$$

as in [4], with $\tau = \tau(t, \mathbf{X}(t))$, $\sigma = \sigma(t, \mathbf{X}(t))$ (with the $\mathbf{X}'(t - \sigma)$ term possibly being zero). The right hand side function $\mathbf{F}$ is defined on $\mathbf{F}$: $[t_0, t_1] \times \mathbb{R}^d \times \mathbb{R}^d \times \mathbb{R}^d \to \mathbb{R}^d$ (in the nonneutral equation case, the third $\mathbb{R}^d$ is nonexistent in this definition of $\mathbf{F}$).

The presence of the delay terms in (3.8) can introduce jump discontinuities in any of the derivatives of $\mathbf{X}$, including in $\mathbf{X}'$. For the initial value DDE problem we are examining, any numerical method that is based on step-by-step continuation of the solution reaches its order of accuracy whenever each step interval is sufficiently smooth. The requirement for a numerical method for solution of DDEs to have order at least k is that the solution must be at least C^{k+1}-continuous on the interval. By this fact, it can be seen that it is

needed for all of the discontinuity points of the y-th derivative of $\mathbf{X}$ to be included in the set of the nodes for the numerical calculations. This must be done for all $y = 0, 1, \ldots, k + 1$.

Most of the properties of the points of discontinuity are determined by the delay arguments of $\mathbf{F}$, i.e. the delays "$t - \tau$" and "$t - \sigma$". In the case that

$$t - \tau \geq t_0 \quad \text{and} \quad t - \sigma \geq t_0 \quad \text{for} \quad all \quad t \geq t_0 , \tag{3.9}$$

the discontinuities do not propagate throughout the solution, and the regularity of the solution depends on only the regularity of $t - \tau, \quad t - \sigma$, and $\mathbf{F}$. As said before, it is generally true that for RFDEs there is "smoothing" of the solution, while for NDDEs this does not occur.

Smoothing of the solution is defined as the following phenomenon. We discuss only the scalar case (i.e. $d = 1$) to briefly demonstrate the definition. We can assume that although the solution continuously joins the given pre-interval solution at time t_0, the first derivative of $\mathbf{X}$ does not exist at the point t_0, because this is what happens for the general DDE initial value problem. (Note that when $\phi, \quad t - \tau$, and $\mathbf{F}$ are each continuous, then so is $\mathbf{X}'$ for any $t \geq t_0$.) If $\phi, \quad t - \tau$, and $\mathbf{F}$ are each differentiable, then $\mathbf{X}'$ exists for all t *except* for the simple roots (if they exist) of the equation

$$t - \tau = t_0, \tag{3.10}$$

as explained in [4]. Each such simple root ρ_i of (3.10) has a jump discontinuity, in $\mathbf{X}''$, at $t = \rho_i$. Each of these jump discontinuities at the ρ_i are called 1-level primary discontinuities. Each of these aforementioned discontinuities creates 2-level primary discontinuities at all of the points ρ'_i which are simple roots of the equation

$$t - \tau = \rho'_i \tag{3.11}$$

for some i. These 2-level primary discontinuities are jump discontinuities in $\mathbf{X}'''$. Likewise, every κ-level primary discontinuity point $\rho^{(\kappa)}_i$ leads to $(\kappa + 1)$-level primary discontinuity points in $\mathbf{X}^{(\kappa+2)}$, the $(\kappa + 2)$-th derivative of $\mathbf{X}$, at successive points $\rho^{(j)}_i$, with the solution $\mathbf{X}$ becoming smoother with each increasing primary discontinuity level. This does *not* occur for neutral DDEs, in which the solution is only guaranteed

to be C^0, i.e. continuous, for each of the primary discontinuity points ρ_i. Some members of the class of non-neutral delay equations may have smoothing occur more quickly than described above at some points, and even some, but not all, delay equations of neutral class have the smoothing property. We will not discuss such properties of NDDEs in detail as this paper is primarily concerned with systems of RFDEs.

To obtain a reliable solution result when modeling, it is neccessary to include the points (at least those of low order κ) of discontinuity in the modeling mesh. The specific systems of equations that are the primary focus of this paper are of constant equal delay, denoted as τ, and therefore all of the discontinuity points in the system are given by $t_0 + k\tau, \ k \in \mathbb{N}$. In our systems being examined, since the delay is always constant, the discontinuity points give an increasing sequence $\rho^{(\kappa)}{}_i, \ \kappa \in \mathbb{N}$, in which $\kappa_1 < \kappa_2$ implies $\rho^{(\kappa_1)}{}_i < \rho^{(\kappa_2)}{}_i$. In this case, we have $\forall \kappa \in \mathbb{N}, \ \rho^{(\kappa)}{}_1$ is the only κ-level discontinuity point.

3.5.1 Sample Existence Results for DDEs (Specifically RFDEs)

If we look first at the time interval $[t_0, t_0 + \min(\tau_0, \sigma_0)]$, then the DDE reduces to

$$
\begin{cases}
\mathbf{X}'(t) = \mathbf{F}\left[t, \ \mathbf{X}(t), \ \phi(t - \tau(t, \mathbf{X}(t))), \ \phi'(t - \sigma(t, \mathbf{X}(t)))\right], & t \geq t_0 \\
\mathbf{X}(t_0) = \phi(t_0),
\end{cases}
\tag{3.12}
$$

on this interval. (3.12) is an ODE and so widely known ODE theorems can be used to prove existence and uniqueness on this interval. We include here a handful of theorems from [4] which are based on theorems stated by Hale, and El'sgol'ts/Norkin.

Theorem 3.5.1. (Local Existence 1) *Consider the equation*

$$
\boldsymbol{X}'(t) = \boldsymbol{F}(t, \boldsymbol{X}(t), \boldsymbol{X}(t - \tau(t))), \quad t_0 \leq t \leq t_f; \quad \boldsymbol{X}(t_0) = \boldsymbol{X}_0,
\tag{3.13}
$$

and assume that the function $\boldsymbol{F}(t, u, v)$ is continuous on $A \subseteq [t_0, t_f) \times \mathbb{R}^d \times \mathbb{R}^d$ and locally Lipschitz continuous with respect to u and v. Also, assume that the delay function $\tau(t) \geq 0$ is continuous in $[t_0, t_f), \tau(t_0) = 0$, and that for some $\xi > 0$, we have $t - \tau(t) > t_0$ in the interval $(t_0, t_0 + \xi]$. Then, the problem (3.13) has a unique solution in $[t_0, t_0 + \delta)$, for some $\delta > 0$ and this solution depends continuously on the initial data.

Under the same assumptions of this theorem, the solution can be continued until some *maximal solution* defined in the interval $[t_0, b)$, with $t_0 < b \leq t_f$. We can use this to prove the following theorem.

Theorem 3.5.2. (Global Existence 1) *If, under the hypotheses of Theorem* (3.5.1)*, the unique maximal solution of* (3.13) *is bounded, then it exists on the entire interval* $[t_0, t_f)$. *In order to apply the global existence theorem, an a priori bound for the solution is required. We can use the following corollary to do this:*

Corollary 3.5.3. *Assume that in addition to the hypothesis of* (3.5.1) *holding, the function* $\boldsymbol{F}(t, u, v)$ *satisfies the condition*

$$||\boldsymbol{F}(t, u, v)|| \leq M(t) + N(t)(||u|| + ||v||) \tag{3.14}$$

in $[t_0, t_f) \times \mathbb{R}^d \times \mathbb{R}^d$, *where* $M(t)$ *and* $N(t)$ *are continuous positive functions on* $[t_0, t_f)$. *Then the solution of* (3.13) *exists and is unique on the entire interval* $[t_0, t_f)$.

This theorem holds in the case of multiple delays, and provides global existence, uniqueness, and continuous dependence on initial data for the solution of the (linear) DDE

$$\begin{cases} \mathbf{X}'(t) = \sum_{i=0}^{r} A_i(t)\mathbf{X}(t - \tau_i(t)) + \mathbf{g}(t), & t \geq t_0 \\ \mathbf{X}(t) = \phi(t), & t \leq t_0, \end{cases} \tag{3.15}$$

for any continuous function $A_i(t)$, $i = 0, 1, \ldots, r$, $\phi(t)$, and $g(t)$ and for any set of continuous delays $\tau_i(t) \geq 0$. [4] The following theorem, under the hypotheses of Thm. (3.5.1), extends existence of a solution to the state-dependent delay case.

Theorem 3.5.4. (Local Existence 2) *Consider the equation*

$$\begin{cases} \boldsymbol{X}'(t) = \boldsymbol{F}[t, \boldsymbol{X}(t), \boldsymbol{X}(t - \tau(t, \boldsymbol{X}(t)))], & t \geq t_0, \\ \boldsymbol{X}(t) = \phi(t), & t \leq t_0. \end{cases} \tag{3.16}$$

Let $U \subseteq \mathbb{R}^d$ *and* $V \subseteq \mathbb{R}^d$ *be neighborhoods of* $\phi(t_0)$ *and* $\phi(t_0 - \tau(t_0, \phi(t_0)))$, *respectively, and assume that the function* $\mathbf{F}(t, u, v)$ *is continuous with respect to* t *and Lipschitz continuous with respect to* u *and* v *in* $[t_0, t_0 + h] \times U \times V$ *for some* $h > 0$. *Also, assume that the initial function* $\phi(t)$ *is Lipschitz continuous*

for $t \leq t_0$ and that the delay function $\tau(t, y) \geq 0$ is continuous with respect to t and Lipschitz continuous with respect to X in $[t_0, t_0 + h] \times U$. Then the problem (3.16) has a unique solution in $[t_0, t_0 + \delta)$ for some $\delta > 0$ and this solution depends continuously on the initial data.

For existence of solution on any finite interval $[t_0, t_0 + \delta]$, one can do integrations on successive intervals of length $\min(\tau_0, \sigma_0)$ one at a time until time $t_0 + \delta$ is reached. Once the solution is known up to the i-th interval, then the solution on the following interval of length $\min(\tau_0, \sigma_0)$ can be found via the above ODE in conjunction with the already computed solution over the previous intervals.

3.6 Characteristic Equation of a DDE: Definition, Purpose, and Obtainment

The characteristic equation of a DDE is obtained in much the same way as for an ODE. Like the characteristic equation of an ODE, the characteristic equation of a DDE can be used to determine stability properties of the equation(s) in question. In the linear discrete delay case, i.e. when working with the system

$$\frac{d}{dt}X(t) = AX(t) + B_0 X(t - \tau_0) + B_1 X(t - \tau_1) + \cdots + B_m X(t - \tau_m), \qquad (3.17)$$

the characteristic equation is

$$\det\left(sI - A - B_0 e^{-s\tau_0} - B_1 e^{-s\tau_1} - \cdots - B_m e^{-s\tau_m}\right) = 0. \qquad (3.18)$$

For cases that are not the linear discrete delay case, the characteristic equation takes a similar form. Together all such characteristic roots s that satisfy Eq. (3.18) are referred to as the *spectrum*. In contrast to the ODE case in which there is a finite spectrum, in the DDE case the spectrum is infinite, i.e. the characteristic equation has an infinite number of characteristic roots s. This is because while the characteristic equation of an ODE is a polynomial, the characteristic equation of a delay system is a quasipolynomial as it contains at least one exponential term.

3.7 Stability In More Detail for the Constant Delay Case

3.7.1 Standard Approach via Continuous ODE Models

For the constant delay case, we consider the equation system:

$$\begin{cases} \mathbf{X}'(t) = \mathbf{F}\left[t,\ \mathbf{X}(t),\ \mathbf{X}(t-\tau)\right]; & t_0 \leq t \leq t_f, \\ \mathbf{X}(t) = \phi(t), & t \leq t_0. \end{cases} \tag{3.19}$$

Overlapping is the case of when the continuous ODE method extension we use makes the overall method implicit despite the particular ODE method being explicit. This is undesirable, and necessitates usage of different algorithms than in the non-overlapping case. To avoid the undesired case we can use small enough step sizes (less than t_0). It is an additional requirement that we need to be able to compute the discontinuity points in advance and use those discontinuity points in the mesh. Specifically, we need to include in the mesh the principal discontinuity points and also the discontinuity points of order less than, for example p, in $[t_0, t_f]$. We denote these discontinuity points by $d_0 = t_0 < d_1 < d_2 < \cdots < d_s$, assuming they have the property that, on each interval $[d_0, d_1], [d_1, d_2], [d_2, d_3], \ldots, [d_s, t_f]$, the solution we want is of class at least C^{p+1}. We also need to have that with $d_{s+1} = t_f$, each $[d_i, d_{i+1}]$ is mapped to the time interval immediately preceding d_i by the previously defined deviated argument, "$t - \tau$". Taking all of this into account, the sequence of ODEs

$$\begin{cases} \mathbf{Y}'(t) = \mathbf{F}\left[t,\ \mathbf{Y}(t),\ \eta(t-\tau)\right]; & d_i \leq t \leq d_{i+1}, \\ \mathbf{Y}(d_i) = \eta(d_i), & t \leq t_0, \end{cases} \tag{3.20}$$

can be solved via a general k-step numerical method [4] and then interpolated for $i = 0, 1, \ldots, s$. η is found on the first interval using the initial function, and then for the successive intervals recursively using the intervals with already found solution.

3.7.2 Stability Analysis of Runge-Kutta Methods for ODEs

Runge-Kutta methods are a widely used one-step method for numerical computation of solutions. R-K methods can be applied to ordinary differential equations of the form:

$$\begin{cases} \mathbf{X}'(t) = G(t, \mathbf{X}(t)) \; ; & t_0 \leq t \leq t_f, \\ \mathbf{X}(t_0) = x_0. \end{cases} \qquad (3.21)$$

The method is employed as follows [4]:

- Choose a step size $h > 0$.

- Define $X_{n+1} = X_n + \frac{1}{6}h(k_1 + 2k_2 + 2k_3 + k_4)$ and $t_{n+1} = t_n + h$ for $n = 0, 1, 2, \ldots$, using

  - $k_1 = G(t_n, X_n)$

  - $k_2 = G(t_n + \frac{h}{2}, X_n + h\frac{k_1}{2})$

  - $k_3 = G(t_n + \frac{h}{2}, X_n + h\frac{k_2}{2})$

  - $k_4 = G(t_n + h, X_n + hk_3)$.

The approximation of $X(t_{n+1})$ is X_{n+1}. Each next value X_{n+1} is found by taking the current value X_n in a weighted average of the four above increments which is based on the product of the step size h with an estimation of the slope of the given function G.

3.7.3 Stability of Linear Periodic Equations

When we have the DDE

$$\mathbf{X}'(t) = G(t)\mathbf{X}_t \; ; \quad t \in \mathbb{R}, \qquad (3.22)$$

with suitable restrictions on $G(t)$ including the condition that $\exists \, \omega > 0$ s.t. $G(t + \omega) = G(t)$ for all $t \in \mathbb{R}$, we have a linear periodic DDE. The operator from $\mathbf{X}$ into itself which assigns the state $\mathbf{X}_t$ at time $t \geq s$ to the initial function $\phi \in \mathbf{X}$ is called the *evolution operator* and is denoted by

$$T(t, s)\phi = \mathbf{X}_t(\bullet; s, \phi). \qquad (3.23)$$

Now, if $T(t, s)$ is this evolution operator associated to (3.22) in the periodic case specifically, then the *monodromy operator* is defined as the operator $Q = T(\omega, 0)$. As expressed in [5], any nonzero element Π in the spectrum of Q is called a *characteristic/Floquet multiplier* of the DDE. Because Π is nonzero, we can

write $\Pi = e^{\omega\lambda}$ with λ being called the characteristic root (or Floquet exponent, if preferred). We have the facts [5] that

Lemma 3.7.1. $\Pi \neq 0$ *is a characteristic multiplier iff.* $\exists \phi \neq 0$ *such that* $Q(t+\omega, 0)\phi = \Pi Q(t, 0)\phi$ *for all* $t \geq 0$.

Lemma 3.7.2. *If* Π *is a characteristic multiplier, then* Π *is an eigenvalue of the operator* $Q(s+\omega, s)$, *for all* $s \in \mathbb{R}$.

In the periodic case, we cannot take the infinitesimal generator approach for finding stability properties, and we must alternatively rely [5] on the following theorem:

Theorem 3.7.3. *The zero solution of (3.22) is uniformly asymptotically stable iff. all the characteristic multipliers of the DDE have complex modulus at most* 1, *i.e. all the characteristic exponents have negative real part. If there are one or more characteristic multipliers with complex modulus greater than* 1, *the system is unstable. Also, the zero solution of (3.22) is uniformly stable iff. all the characteristic multipliers of the DDE have modulus* ≤ 1 *and if* Π *is a multiplier with modulus equal to* 1 *then all the solutions in the associated eigenspace are bounded.*

3.7.4 Linear Autonomous RFDEs

Linear autonomous RFDEs are linear RFDEs that are time translation invariant. More specifically, if

$$x_t(\theta) := [x(t+\theta), \; -h \leq \theta \leq 0] \tag{3.24}$$

satisfies $x_t(\theta) \in C([-h, 0], \mathbb{C}^n)$, and L is a continuous linear mapping from $C([-h, 0], \mathbb{C}^n)$ into $\mathbb{C}^n$, then $\dot{x}(t) = Lx_t$ is a linear autonomous RFDE [12]. If all of the time delays in the system are constant, then [4, 27] the system is at once an autonomous one. Therefore, linear delay systems with constant delays are always linear autonomous RFDEs. When we have a linear autonomous system, the consequences of the Riesz representation theorem:

Theorem 3.7.4. *If* $\mathcal{H}$ *is a Hilbert space whose inner product* $\langle x, y \rangle$ *is linear in its first argument and antilinear in its second argument, then for every continuous linear functional* $\phi \in \mathcal{H}^*$, *there exists a unique*

$f_\phi \in \mathcal{H}$ *such that*

$$\phi(x) = \langle x, f_\phi \rangle \quad \textit{for all } x \in \mathcal{H}. \tag{3.25}$$

(If $\mathcal{H}$ is a complex Hilbert space, the vector $f_\phi \in \mathcal{H}$ is always located in the antilinear coordinate of the inner product.) It also follows that $||f_\phi||_{\mathcal{H}} = ||f_\phi||_{\mathcal{H}^*}$ and f_ϕ is the unique vector in $\mathcal{H}$ satisfying $f_\phi \in (\ker \phi)^\perp$ and $\phi(f_\phi) = ||\phi||^2$, with $\perp$ defined as the orthogonal complement of a subset. If $k \in (ker\phi)^\perp$ is nonzero then $\phi(k) \neq 0$ and $k = \frac{||k||^2}{\phi(k)} f_\phi$. Additionally, f_ϕ is the unique element of minimum norm in $C := \phi^{-1}(||\phi||^2)$, i.e. f_ϕ is the unique element of C that satisfies $||f_\phi|| = \inf_{c \in C} ||c||$,

give that if L is a mapping as given in the preceding, then there exists a unique function of normalized bounded variation that can be used when working with the RFDEs in question. The reader is referred to the first part of Chapter 1 of [12] for the details.

With an RFDE of the form

$$\dot{x}(t) = \int_0^h d\zeta(\theta) x(t - \theta), \tag{3.26}$$

with ζ being a given function of normalized bounded variation, i.e., $\zeta \in \text{NBV}([0, h], \mathbb{C}^{n \times n})$ given, the system can be written as a *renewal equation* for x as follows. First, write Eq. (3.26) in the form

$$\begin{cases} \dot{x}(t) = \int_0^t \zeta(\theta)\dot{x}(t - \theta)d\theta + g(t), \\ x(0) = \phi(0), \\ \\ g(t) := \zeta(t)\phi(0) + \int_t^h d\zeta(\theta)\phi(t - \theta). \end{cases} \tag{3.27}$$

A renewal equation is an equation of the form $x = \zeta * x + f$, with $*$ denoting the standard convolution product and x being the unknown function. (3.27) is a renewal equation (alternatively called a *Volterra convolution integral equation*), for $\dot{x}$. Note that $g(t)$ as defined in the preceding is continuous. [12] Integrating, we get from (3.27)

$$x = \zeta * x + f_r, \tag{3.28}$$

with

$$f_r(t) = \phi(0) + \int_0^t \left(\int_s^h d\zeta(\theta)\phi(s - \theta) \right) ds, \tag{3.29}$$

45

which is a renewal equation now for x instead of for $\dot{x}$.

The *characteristic matrix* $\Delta(\lambda_z)$ of the delay system (3.26) determines the stability properties of the system and is given by, for complex λ_z,

$$\Delta(\lambda_z) = \lambda_z I - \int_0^h e^{-\lambda_z t} d\zeta(t). \tag{3.30}$$

As proven in the first chapter of [12], the renewal equation (3.28) corresponding to the delay equation (3.26) has its solution for $t > 0$ given by

$$x(t) = \frac{1}{2\pi i} \int_{L(\gamma)} e^{\lambda_z t} \Delta(\lambda_z)^{-1} (f_r(0) + \int_0^h e^{\lambda_z \theta} df_r(\theta)) d\lambda_z , \tag{3.31}$$

for $\gamma > \sup\left(\Re(\lambda_z) : \det \Delta(\lambda_z) = 0\right)$.

3.7.5   *Stability of Linear Autonomous RFDEs*

If the determinant of $\Delta(\lambda_z)$ has no zeros in λ_z with positive real part, then all solutions of the RFDE (3.26) converge to zero exponentially as $t \to \infty$.

3.7.6   *Stability Analysis of DDEs*

The main goal of performing analysis on any type of delay differential equation system is most often to find system parameters guaranteeing stability (in some cases, instability instead is desired) of the system under consideration. This is done for system parameters which can be usefully controlled in application of the system in question to some real-world process or machine. In general, this process involves analyzing stability of the zero solution of a system. This is standard because one may consider the delay equation corresponding to the zero initial function, which reduces stability analysis of the system to stability analysis of the zero solution [5]. Once parameters guaranteeing stability (resp. instability) are found, the system is then converted back into having the actual initial conditions of the specific application.

The most commonly used methods of stability analysis for delay equations are divided into two classes depending on whether or not stability for *all* constant delays is sought. For the system being examined, if this additional outcome is desired, the system analyst is concerned with finding conditions under which *delay-independent stability* holds. If this stronger constraint on the system parameters is not needed,

then the other of these two classes of methods, which is based on finding conditions which guarantee *delay-dependent stability*, can be used. These two terms have self-evident definitions. In the scalar DDE case

$$x'(t) = \alpha x(t) + \beta x(t - \tau),\tag{3.32}$$

the study of stability regions for fixed delay τ has been exhausted for $\alpha, \beta \in [\mathbb{R} \cup \mathbb{C}]$ [4]. There are many different methods for doing delay-independent analysis, and many as well for doing delay-dependent analysis. The conditions for having delay-independent stability are clearly stricter than those for having delay-dependent stability.

3.7.7 Stability Analysis of Runge-Kutta (RK) Methods for DDEs

The reader is referred to the last few pages of Ch. 10 of [4] for the Runge-Kutta formula for constant delay DDEs and more specifics on using it for stability analysis.

3.8 Summary of Linear RFDEs as Bounded Perturbations

The general idea of this method is that if there is a linear autonomous RFDE, such an equation can be represented in a more abstract way: Consider a system originally in the form

$$\dot{x}(t) = \int_0^h d\zeta(\theta)x(t - \theta), \quad t \geq 0 \text{ and } x(t) \in \mathbb{C}^m,\tag{3.33}$$

with ζ being a $m \times m$ matrix-valued function whose entries are of normalized bounded variation. This system can be written as a differential equation made up of two components: a *shifting* component and an *extending* component. The two components, defined as such in [12], are independent of each other. The chosen operator describing the extension component of the equation is both linear and bounded. Then, the system equation as written in this new form is formally integrated, which yields a variation-of-constants equation. The first component of this variation-of-constants equation can then be used to find the unique solution of (3.33) given some specified initial condition. The concept of the *weak* integral* is used in this process. For more information on this method, the reader is referred to Chapter 3 of [12].

3.9 More Information Applicable to Either Linear or Non-linear RFDEs

In finding the solution of a RFDE, one may need to find a way to extend the solution in order to obtain the solution for arbitrary positive time. In fact, in order to construct solution operators for a RFDE one requires both a way of extending the solution and a method of shifting the function back to previous "segments" of the solution. The initial "segment" is the function defined a priori on an interval $[-h, 0]$ for some positive h. [12] When working with a delay differential equation, this given function on the interval $[-h, 0]$ is also known as the initial state. The *state at time* t is the piece of the extended solution defined on the interval of length h of $[t - h, t]$. It happens that although the method of extending the solution function is different for each specific equation, the method of shifting back to the previous piece of the solution is the same for *all* DDEs. We will not go into details here, but the inquisitive reader is referred to Chapter 2 of [12] for an explanation of the shift-semigroup based approach of working with linear or nonlinear DDEs.

3.10 Numerical Analysis Methods

3.10.1 SO Method

The solution operator numerical method, or *SO method*, approximates the eigenvalues of an evolution operator $\Omega := \Omega(s + h, s) : \mathbf{X} \to \mathbf{X}$, for a DDE system

$$\mathbf{X}'(t) = F(t, \mathbf{X}(t), \mathbf{X}(t - \tau(t))). \tag{3.34}$$

The approximations are based on the eigenvalues of a finite-dimensional approximation of Ω. An overview of this method and specifics can be found in [5], Chapter 6.

3.10.2 IG Approach

The infinitesimal generator approach is one such method for finding stable and unstable parameter combinations, i.e. stable and unstable regions in the parameter space, of a delay equation system. The IG approach is a relatively broad class of methods and includes:

- the pseudospectral differentiation method

- the piecewise version of the pseudospectral differentiation method and

- *any* method of discretizing a derivative based on Runge-Kutta methods

- *any* method of discretizing a derivative based on linear multistep methods, although this sub-class of methods is generally not used due in part to a slower order of convergence of the discrete characteristic root approximations to the continuous characteristic roots.

The pseudospectral differentiation method and its piecewise analogue are usually preferred for these purposes, because [5] of their faster convergence.

No matter which subclass of the infinitesimal generator method is used, it involves approximating the space $\mathbf{X}(t)$ with a finite-dimensional linear space, say $\mathbf{X}_M$. The finite-dimensional approximation of the space is termed the *discretization of X of index M*. We have a (linear, autonomous) delay DE

$$x'(t) = Lx_t , \tag{3.35}$$

with L being a bounded, linear functional taking $\mathbf{X}$ into $\mathbb{C}^d$ for some integer d. (3.35) may be reformulated as an abstract ODE in $\mathbf{X}$, the (infinite-dimensional) space as follows:

$$y'(t) = \Omega y(t), \tag{3.36}$$

with Ω being the infinitesimal generator of the SO semigroup $\{T(t)\}_{t\geq 0}$, as described in the reference. Here, $y(t) = x_t$. Continuing as in [5], it is required that we approximate the infinitesimal generator Ω with a finite-dimensional, linear operator Ω_M which maps $\mathbf{X}_M$ into itself. Ω_M is called the *discretization of Ω of index M*. By definition, larger values of M correspond to increased accuracy in approximating $\mathbf{X}$ and Ω. Finally, the characteristic roots of the DDE system are approximated by finding the eigenvalues of the discretization Ω_M. The pseudospectral differentiation method and the piecewise pseudospectral differentiation method are both covered in detail in [5], and in this paper we instead use the Lambert W function method.

Chapter 4

Main Results

4.1 Introduction

In this section, which contains our analysis, we plot selected graphs of stable and unstable regions for each of the coupled systems we are modeling. We take our delay terms to be the mass or cantilever function representing one of our cantilevers without delay, but at the time $t - \tau$, with t being the current time in the system. Within each equation model, we use the same delay time τ for both of the feedback loops.

4.2 Summary of MATLAB Program and Toolkit Used

To obtain accurate graphs of stable and unstable regions, we employ the "QPMR toolbox" as described in [18, 24, 23, 25] to find the stability exponent for a given gain-gain-delay combination. We then plot the resulting values with a contour fill plot for convenient choices of contour levels. We plot the stability exponent points in one gain-delay plane with the other of the two gain values fixed. We then repeat the process with various different values for the fixed gain, obtaining multiple contour plots in the process. In this way we can examine trends in the existence and behavior of stable regions as the parameters are varied.

For the purposes of quicker searching for stable region parameter combinations when finesse is not needed, the author has written a small MATLAB algorithm based on the Lambert W-function. This program can be used to obtain an idea of the stable and unstable regions in much less computational time than via using the QPMR program, or to obtain a much finer plotted grid in the same amount of time. The code can be provided upon request.

4.3 Harmonic Oscillator Verification

The following stability maps for a rudimentary harmonic oscillator were created using the QPMR toolkit as a verification of proper functionality. Note that these are known cases. A handful of stability graphs for one simple harmonic oscillator in a delayed feedback system is as follows. As $\tau \to \infty$ the case of a single harmonic oscillator results in a negative stability exponent whenever there is positive or no damping, as expected. Figure (6a) is verified to match the known graph in [17] and is this case with varying, non-extremal τ.

As delay time $\tau \to \infty$, it is clear that the stability properties of the corresponding coupled harmonic oscillator system will mimic the stability properties of *uncoupled* harmonic oscillators. Therefore, we can omit the graphs for this case and say that as $\tau \to \infty$ the system is stable whenever both of the components are stable, i.e. whenever both of the harmonic oscillators in the system have either positive or no damping.

For either values γ used in the graphs (3a) and (16b), analysis of the limiting case as the delay time $\tau \to 0$ yields instability for all gain values G_i if we use the same physical constants as in all the preceding plots.
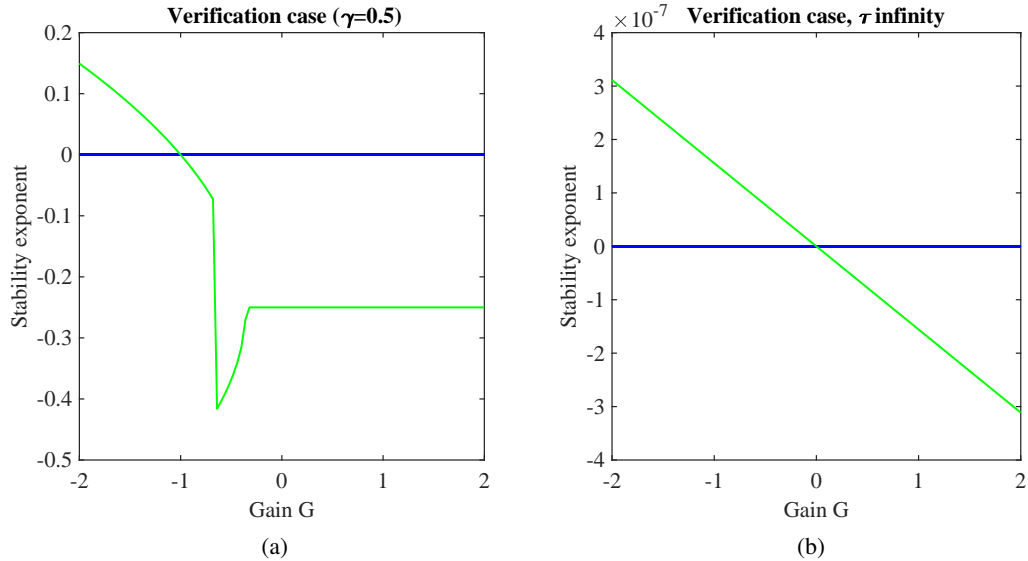
Figure 2.: Single harmonic oscillator. (a) Stability plot for verification for $\tau = 0$. Stability holds for all gain $G \geq -1$. (b) Delay time $\tau \to \infty$, for verification. The system is stable for all positive gain G.

(a)

(b)
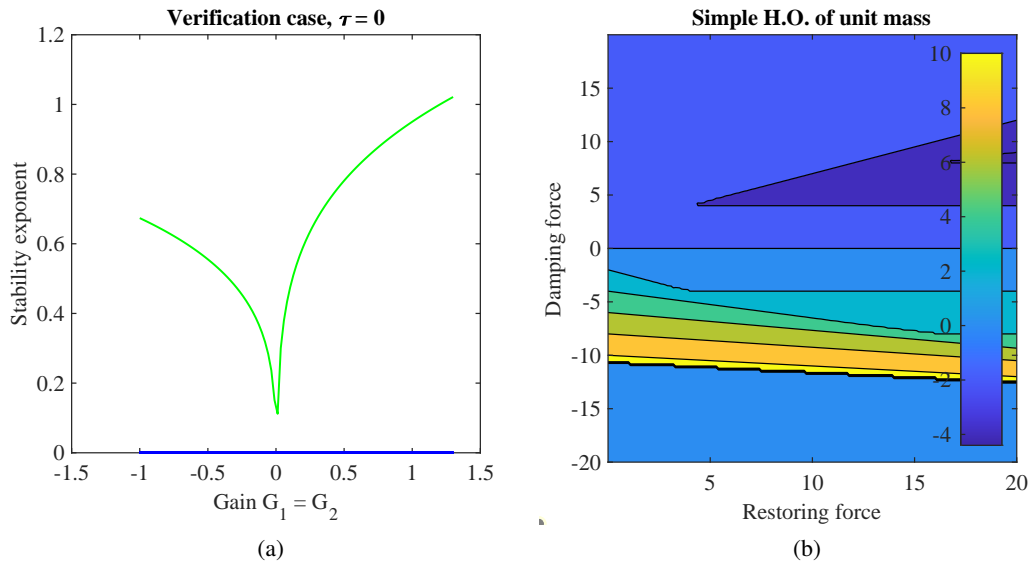
Figure 3.: (a) Coupled harmonic oscillators' stability plot for $\tau = 0$, for verification. This plot is unstable for any nonzero gain values G_1, G_2 that have $G_1 = G_2$. (b) One simple harmonic oscillator in the k, γ-plane, i.e. the restoring force, damping force plane. Note that the upper half plane is stable, while on the other hand, the lower half plane is unstable. This graph corresponds to the fact that [10] a simple harmonic oscillator is stable exactly when there is either positive damping or zero damping.

We also, in Fig (4), verify graphs from [15].

(a)

(b)
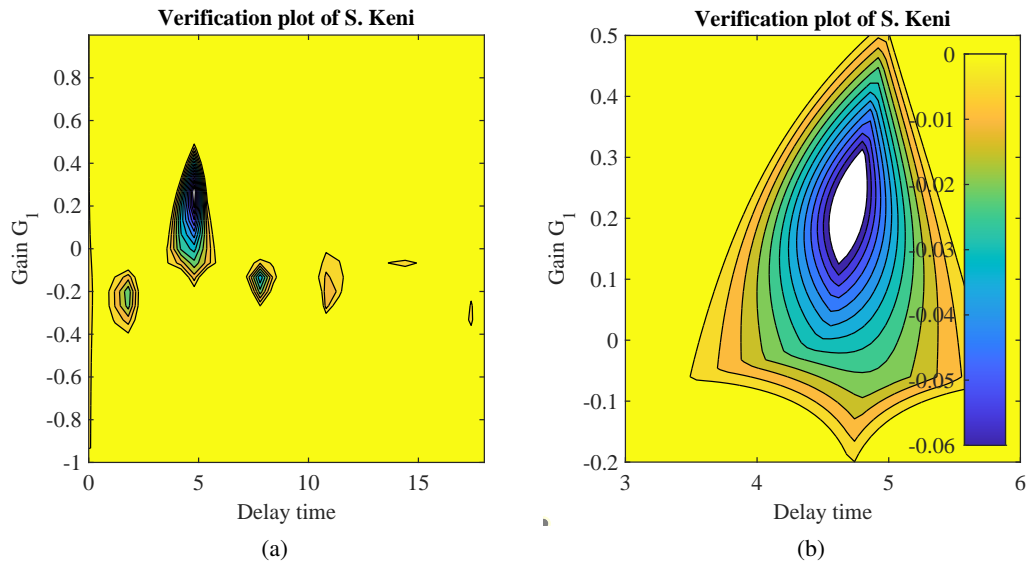
Figure 4.: (a) Our program-generated verification graph of [15] p. 53. Yellow is unstable. (b) Zoom in of verification graph of [15] p. 53 on a stable region.

4.4 Beam Equation With Delay Verification

Note that the single beam equation with delay is a known case. Because the beam equation is closer to being a partial differential equation than the harmonic oscillator's ODE case we are examining, when dealing with the beam equation an additional variable is introduced into the stability plot from the Fourier transform. We denote this Fourier transform variable $x \rightarrow p$.

4.4.1 *Eighth Order System's Verification (for the cases $\tau \rightarrow 0$ and $\tau \rightarrow \infty$)*

These limiting cases are included here to test that our program set is running correctly. When delay time tends to infinity, the exponential term disappears and the stability exponent is a constant positive number for arbitrary gain ratio. This results in the system always being unstable. On the other hand, when the delay time tends to zero, we get one stable area, which depends only on the gain ratio.

4.4.2 *Additional Verification*

We verify some of the plots from [17] for additional confirmation that our program setup works properly. Figures (6a), (6b), and (18) are all in accordance with the corresponding plots in [17].

4.5 Pair of Coupled Harmonic Oscillators With Delay

The first considered model in this paper is a delay-coupled pair of harmonic oscillators. The investigated model in [15] consists of the equivalent of having each of the two masses in a line, connected by a spring between them and a spring on either side of the plant, with the separate delay feedback being the forcing of a previous time state of each spring mass on its own current state. In contrast, our model has the two spring masses being isolated from each other except for the delay forcing. In our system, the past position of each spring mass, via a piezoelectric bimorph influences only the other mass and not itself. Like [15], we assume that the time delays are the same throughout the system. After normalization of our coupled system of equations, our system is given by

$$\begin{cases} \frac{d}{dt^2} Z_1(t_c\bar{t}) + \frac{\gamma}{\sqrt{mk}} \frac{d}{dt} Z_1(t_c\bar{t}) + Z_1(t_c\bar{t}) = -G_2 Z_2(t_c\bar{t} - \tau) \\ \frac{d}{dt^2} Z_2(t_c\bar{t}) + \frac{\gamma}{\sqrt{mk}} \frac{d}{dt} Z_2(t_c\bar{t}) + Z_2(t_c\bar{t}) = -G_1 Z_1(t_c\bar{t} - \tau). \end{cases} \quad (4.1)$$
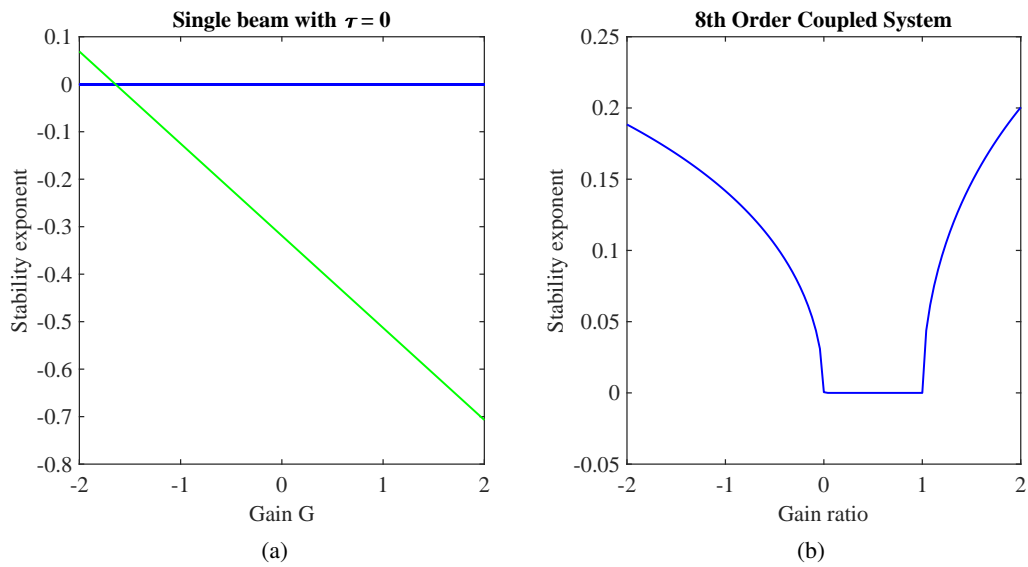
Figure 5.: (a) Single beam with delay τ stability plot for verification with $\tau = 0$, $\gamma = 0.5$, $p = 0.5$. As p increases, the stability region increases its size in the negative direction on the G axis. (b) 8th order coupled beam system stability map, with delay time being held constant at zero. The system is stable for gain ratio between 0 and 1. The stability exponent in that interval is very small and negative.
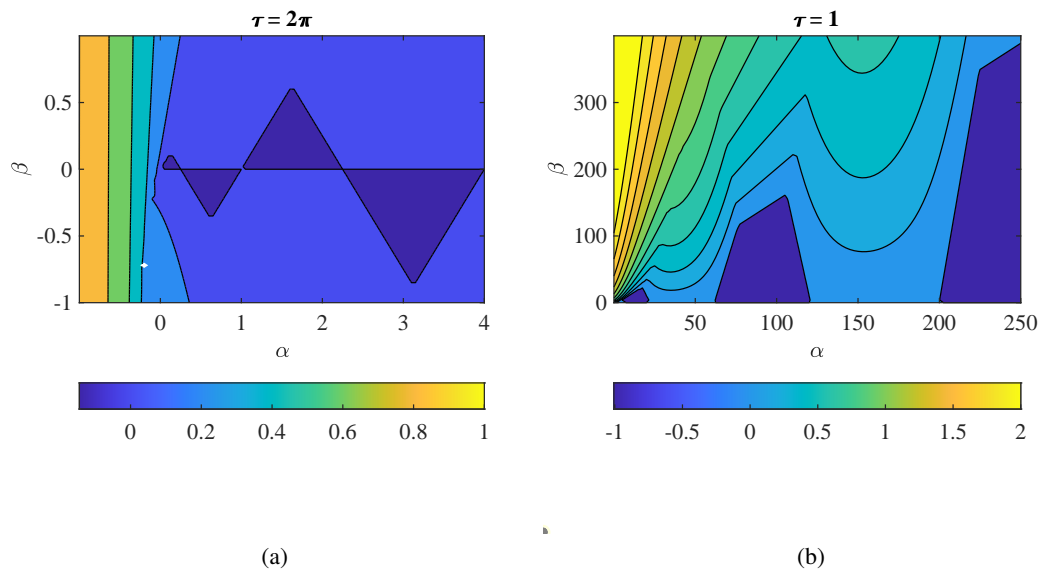

Figure 6.: (a) Verification for autonomous 2nd order system plot in [17], Fig. 3. The darkest blue area is stable. (b) Verification for autonomous 3rd order system plot in [17], Fig. 4. The darkest blue area is stable.

In the system, m is the mass amount, k is the spring constant, γ is the damping term, τ is the time delay, which like in [15] we assume to be the same throughout the system. Also, G_1, G_2 are the gain coefficients which are also the coupling constants, and t_c is the characteristic time value of the normalization.

To graph stability in the gain-delay plane, we fix a gain value G_2 and graph the stability exponent in the τ, G_1-plane. Then we repeat the process for various different fixed values of G_2. We will instead of normalization (4.1), use the normalized equations found in [15], but with our type of coupling, graphing the following system of coupled harmonic oscillators:

$$\begin{cases} \frac{d}{dt^2} Z_1 + \mu \frac{d}{dt} Z_1 + (\omega^2 + k)Z_1 = -G_2 Z_2(t - \tau) \\ \frac{d}{dt^2} Z_2 + \mu \frac{d}{dt} Z_2 + (\omega^2 + k)Z_2 = -G_1 Z_1(t - \tau), \end{cases} \tag{4.2}$$

with $\mu = 0.005$, $\omega = 1$, and $k = 0.1$.

The graphing procedure for the coupled harmonic oscillators for G_2 varying from 0.1 to 1.0 yielded only isolated pockets of stability that appear to be roughly periodic over τ. Stability occurs for only small values of G_1 and these pockets die out as $|G_1|$ increases. Note that the equations are symmetric, i.e. we obtain the same graphs if we switch the values of G_1 and G_2 and plot G_2 as the vertical axis.

As one of the gains (for example G_2) starts from zero and increases to 1, we begin with the whole plane being stable and the introduction of any positive value of G_2 immediately introduces periodic, unstable U-shaped regions that continue vertically to infinity, and they alternate flipping across the tau axis. As G_2 increases to 1.0, the U-shaped unstable regions expand more and more into the tau axis but each U-shape appears to keep its same axis of symmetry and the same position on the tau axis.

4.6 Pair of Cross-Coupled Beam Cantilevers With Delay

Normalization of the coupled beam equation results in the following:

$$\begin{cases} \frac{\partial^4 Z_1(x_c\bar{x}, t_c\bar{t})}{\partial \bar{x}^4} + \frac{\partial^2 Z_1(x_c\bar{x}, t_c\bar{t})}{\partial \bar{t}^2} + \frac{\gamma}{\sqrt{\mu}} \frac{\partial Z_1(x_c\bar{x}, t_c\bar{t})}{\partial \bar{t}} + k_1 Z_1(x_c\bar{x}, t_c\bar{t}) = -k_2 G_2 Z_2(x_c\bar{x}, t_c\bar{t} - \tau) \\ \frac{\partial^4 Z_2(x_c\bar{x}, t_c\bar{t})}{\partial \bar{x}^4} + \frac{\partial^2 Z_2(x_c\bar{x}, t_c\bar{t})}{\partial \bar{t}^2} + \frac{\gamma}{\sqrt{\mu}} \frac{\partial Z_2(x_c\bar{x}, t_c\bar{t})}{\partial \bar{t}} + k_1 Z_2(x_c\bar{x}, t_c\bar{t}) = -k_2 G_1 Z_1(x_c\bar{x}, t_c\bar{t} - \tau). \end{cases} \tag{4.3}$$
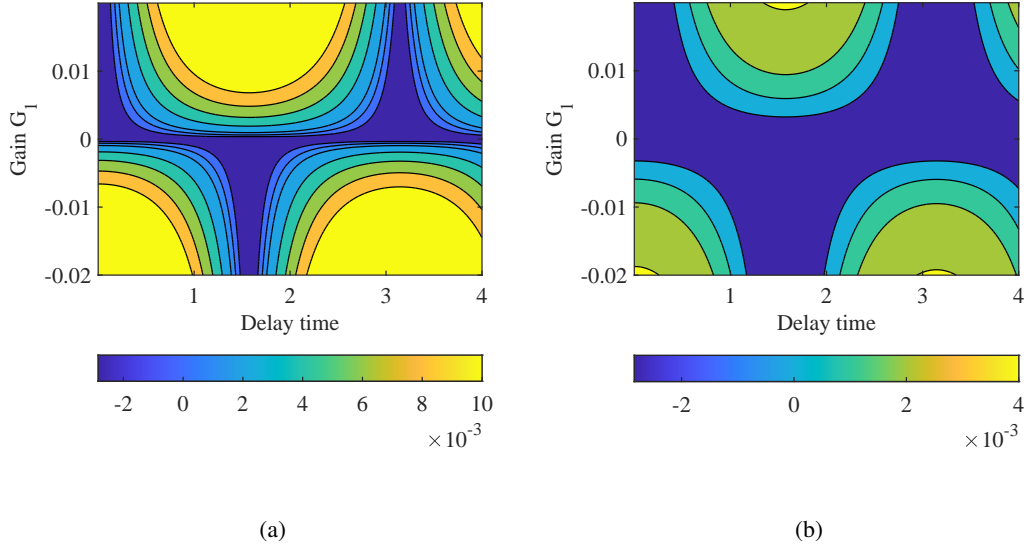
Figure 7.: (a) Stability exponent map of coupled harmonic oscillators for $G_2 = 0.1$. The darkest blue area is stable and all other colors are unstable. Zoomed in region of Figure 19a. (b) Stability exponent map of coupled harmonic oscillators for $G_2 = 0.01$. Darkest blue area is stable.

The characteristic quasipolynomial of the coupled beam system with $k_1 = k_2$ is:

$$(s(s + \frac{\gamma}{\sqrt{\mu}}))^2 + 2(p^4 + k)s(s + \frac{\gamma}{\sqrt{\mu}}) + (p^4 + k)^2 - k^2 G_1 G_2 e^{-2s\tau}, \tag{4.4}$$

or equivalently,

$$(s(s + \frac{\gamma}{\sqrt{\mu}}) + p^4 + k)^2 - k^2 G_1 G_2 e^{-2s\tau}. \tag{4.5}$$

For computational reasons we will instead consider only the following cross-coupled beam system with coefficients similar in magnitude to the coefficients in [15]. The systems (4.3) and (4.6) are physically equivalent, and only differ by the magnitudes of some of their coefficients. The coefficients we will use for our cantilever modeling are $\frac{\gamma}{\sqrt{\mu}} = 0.005,\ k_1 = 0.6,\ k_2 = 0.1$:

$$\begin{cases} \frac{\partial^4 Z_1(x_c\bar{x},t_c\bar{t})}{\partial \bar{x}^4} + \frac{\partial^2 Z_1(x_c\bar{x},t_c\bar{t})}{\partial \bar{t}^2} + 0.005\,\frac{\partial Z_1(x_c\bar{x},t_c\bar{t})}{\partial \bar{t}} + 0.6\,Z_1(x_c\bar{x},t_c\bar{t}) = -0.1\,G_2 Z_2(x_c\bar{x},t_c\bar{t}-\tau) \\ \frac{\partial^4 Z_2(x_c\bar{x},t_c\bar{t})}{\partial \bar{x}^4} + \frac{\partial^2 Z_2(x_c\bar{x},t_c\bar{t})}{\partial \bar{t}^2} + 0.005\,\frac{\partial Z_2(x_c\bar{x},t_c\bar{t})}{\partial \bar{t}} + 0.6\,Z_2(x_c\bar{x},t_c\bar{t}) = -0.1\,G_1 Z_1(x_c\bar{x},t_c\bar{t}-\tau). \end{cases} \tag{4.6}$$

We derive the characteristic quasipolynomial by following the same process as outlined in [14]:

We first take the Fourier transform in x only. For $i = 1, 2$

$$\hat{W}_i(p, t) = \frac{1}{\sqrt{2\pi}} \int_{-\infty}^{\infty} W_i(x, t) e^{-ipx} dx \,, \tag{4.7}$$

Yielding the system

$$\begin{cases} p^4 \hat{W}_1 + \frac{d^2 \hat{W}_1}{dt^2} + 0.005 \frac{d\hat{W}_1}{dt} + 0.6 \hat{W}_1 = -0.1 G_2 \hat{W}_2(t - \tau) \\ p^4 \hat{W}_2 + \frac{d^2 \hat{W}_2}{dt^2} + 0.005 \frac{d\hat{W}_2}{dt} + 0.6 \hat{W}_2 = -0.1 G_1 \hat{W}_1(t - \tau) \,. \end{cases} \tag{4.8}$$

We now write this system of equations as a linear system

$$\dot{\mathbf{X}}(p, t) = \mathbf{A}\mathbf{X}(p, t) + \mathbf{G}_i \mathbf{X}(p; t - \tau). \tag{4.9}$$

The Laplace transform

$$F(s) := \mathcal{L}[f](s) = \int_0^\infty e^{-st} f(t) dt, \tag{4.10}$$

applied to our system of equations gives

$$\mathbf{X} = (s\mathbf{I} - \mathbf{A} - \mathbf{G}_i e^{-s\tau})^{-1} \mathbf{X}(0), \tag{4.11}$$

and the characteristic equation of the system [14] is

$$\Delta = \det (s\mathbf{I} - \mathbf{A} - \mathbf{G}_i e^{-s\tau}), \tag{4.12}$$

$$\Delta = s^4 + 0.01 s^3 + (2p^4 + 1.200025)s^2 + (0.01p^4 + 0.006)s + p^8 + 1.2p^4 + 0.36 - 0.01 G_1 G_2 e^{-2s\tau} \tag{4.13}$$

in the case of our specific system. We plot stability for various fixed values of p.
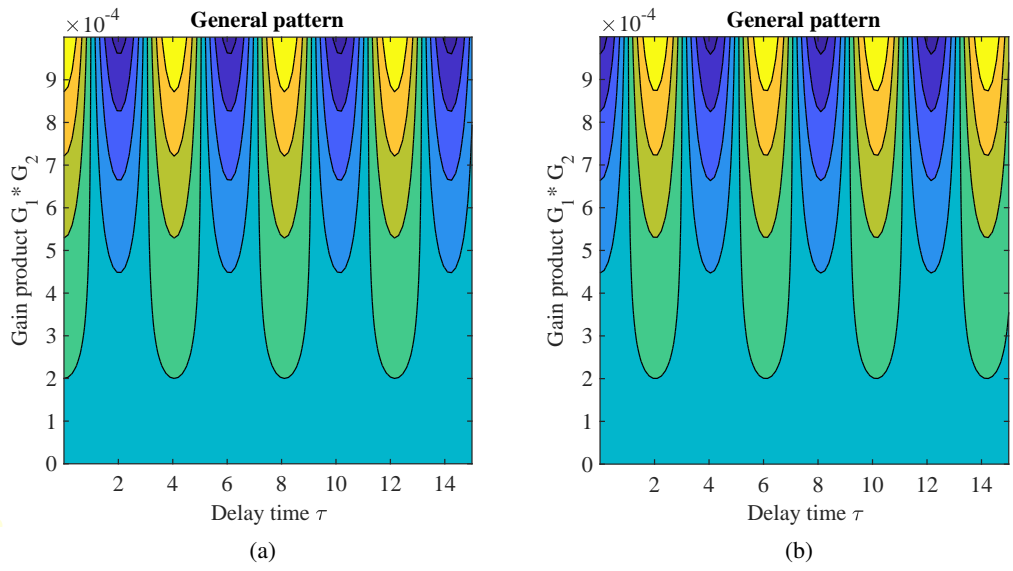
Figure 8.: (a) General pattern of the stability contours of cross-coupled cantilevers for *negative* product of gains, in the same window range as plot b. Here, going vertically upward corresponds to increasing magnitude of *negative* gain product. (b) General pattern of the stability contours, positive product of gains, cross-coupled cantilevers.
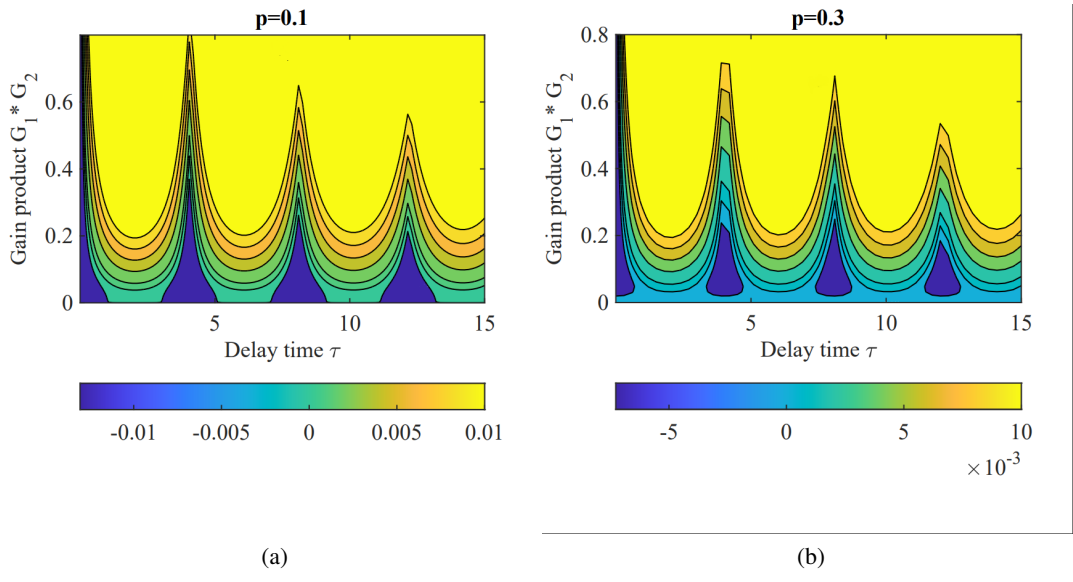
Figure 9.: (a) Cross-coupled cantilevers. Darkest blue is stable, p=0.1. (b) Cross-coupled cantilevers. Darkest blue is stable, p=0.3.
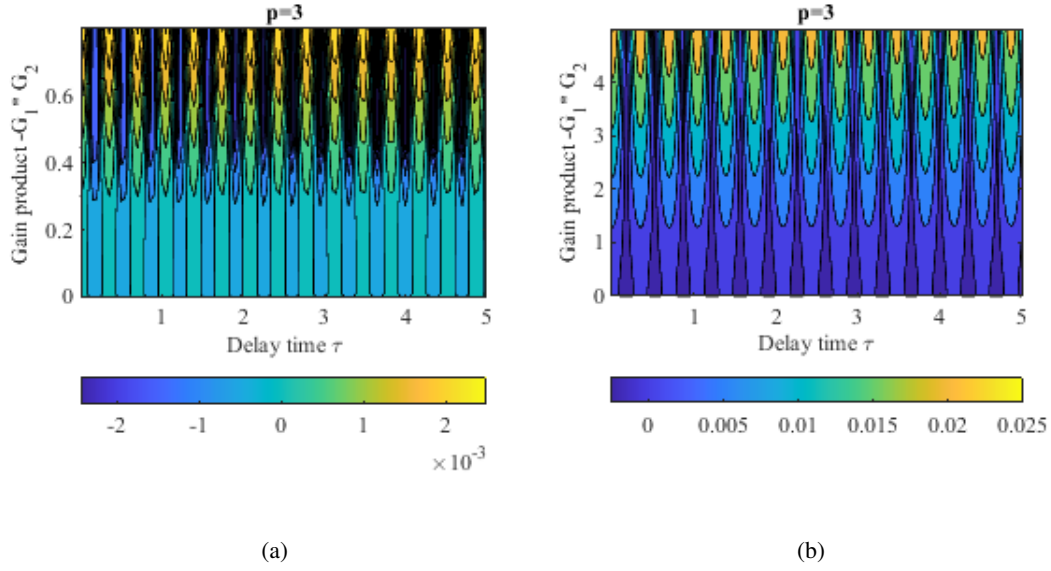
Figure 10.: (a) Cross-coupled cantilevers. Vertical bands of equal period regions alternate between stability and instability when moving along the horizontal τ axis. Graph is with negative gain product and p=3.0 (b) Upon plotting a wider range of the gain product in more detail, it can be seen that what appeared to be vertical strips in Figs. (10a, 26a) are in fact regions that taper off and possibly vanish as gain product increases in magnitude. Here p=3.0 and $G_1 G_2 \leq 0$.

4.7 Conclusion for Cross-Delay Coupled Cantilevers

Many of the stability plots obtained for the cross-coupled beam equation system are quite similar in nature to the stability plots of the single beam equation system in [20]. Switching the sign of the gain in the single beam equation case has the same effect on the stability graphs as switching the sign of exactly one of the gains G_i in our cross-coupled beam case. In particular, switching exactly one of the signs shifts the stable/unstable regions by moving the stability regions to the right or left along the τ axis, as changing the sign of the gain did in the earlier microcantilever paper [20]. This is illustrated in Figs. (8a, 8b).

4.8 Pair of Self-Delay Coupled Beam Cantilevers

The beam equation applied to the setup of [15] yields the normalized system

$$
\begin{cases}
\frac{\partial^4 Z_1(x_c\bar{x}, t_c\bar{t})}{\partial \bar{x}^4} + \frac{\partial^2 Z_1(x_c\bar{x}, t_c\bar{t})}{\partial \bar{t}^2} + \frac{\gamma}{\sqrt{\mu}}\frac{\partial Z_1(x_c\bar{x}, t_c\bar{t})}{\partial \bar{t}} + kZ_2(x_c\bar{x}, t_c\bar{t}) = -kG_1 Z_1(x_c\bar{x}, t_c\bar{t} - \tau) \\
\frac{\partial^4 Z_2(x_c\bar{x}, t_c\bar{t})}{\partial \bar{x}^4} + \frac{\partial^2 Z_2(x_c\bar{x}, t_c\bar{t})}{\partial \bar{t}^2} + \frac{\gamma}{\sqrt{\mu}}\frac{\partial Z_2(x_c\bar{x}, t_c\bar{t})}{\partial \bar{t}} + kZ_1(x_c\bar{x}, t_c\bar{t}) = -kG_2 Z_2(x_c\bar{x}, t_c\bar{t} - \tau).
\end{cases}
\tag{4.14}
$$

59

The CQP of the system

$$\begin{cases} \frac{\partial^4 Z_1(x,t)}{\partial x^4} + \mu\frac{\partial^2 Z_1(x,t)}{\partial t^2} + \gamma\frac{\partial Z_1(x,t)}{\partial t} + kZ_2(x,t) = -kG_1 Z_1(x, t-\tau) \\ \frac{\partial^4 Z_2(x,t)}{\partial x^4} + \mu\frac{\partial^2 Z_2(x,t)}{\partial t^2} + \gamma\frac{\partial Z_2(x,t)}{\partial t} + kZ_1(x,t) = -kG_2 Z_2(x, t-\tau), \end{cases} \quad (4.15)$$

can be obtained by the following process. Letting $Z_i(x,t) = e^{\omega t}Y_i(x)$, $i = 1, 2$; our system is now:

$$\begin{cases} e^{\omega t}Y_1{}^{(4)}(x) + \mu\omega^2 e^{\omega t}Y_1(x) + \gamma\omega e^{\omega t}Y_1(x) + ke^{\omega t}Y_2(x) = -kG_1 e^{\omega(t-\tau)}Y_1(x) \\ e^{\omega t}Y_2{}^{(4)}(x) + \mu\omega^2 e^{\omega t}Y_2(x) + \gamma\omega e^{\omega t}Y_2(x) + ke^{\omega t}Y_1(x) = -kG_2 e^{\omega(t-\tau)}Y_2(x) \end{cases} \quad (4.16)$$

$$\implies \begin{cases} Y_1{}^{(4)}(x) + \mu\omega^2 Y_1(x) + \gamma\omega Y_1(x) + kY_2(x) = -kG_1 e^{-\omega\tau}Y_1(x) \\ Y_2{}^{(4)}(x) + \mu\omega^2 Y_2(x) + \gamma\omega Y_2(x) + kY_1(x) = -kG_2 e^{-\omega\tau}Y_2(x). \end{cases} \quad (4.17)$$

Allow $X_1 := Y_1$, $X_2 := Y_1''$, $X_3 := Y_2$, $X_4 := Y_2''$. So we have

$$\implies \begin{cases} X_2''(x) + (\mu\omega^2 + \gamma\omega)X_1(x) + kX_3(x) = -kG_1 e^{-\omega\tau}X_1(x) \\ X_4''(x) + (\mu\omega^2 + \gamma\omega)X_3(x) + kX_1(x) = -kG_2 e^{-\omega\tau}X_3(x) \end{cases} \quad (4.18)$$

$$\implies \begin{cases} X_1'' = X_2 \\ X_2'' = (-\mu\omega^2 - \gamma\omega - kG_1 e^{-\omega\tau})X_1 - kX_3 \\ X_3'' = X_4 \\ X_4'' = (-\mu\omega^2 - \gamma\omega - kG_2 e^{-\omega\tau})X_3 - kX_1. \end{cases} \quad (4.19)$$

With the coefficient matrix $\mathbf{A}$ of the system:

$$\begin{bmatrix} 0 & 1 & 0 & 0 \\ -\mu\omega^2 - \gamma\omega - kG_1e^{-\omega\tau} & 0 & -k & 0 \\ 0 & 0 & 0 & 1 \\ -k & 0 & -\mu\omega^2 - \gamma\omega - kG_2e^{-\omega\tau} & 0 \end{bmatrix},$$

the characteristic quasipolynomial corresponding to the coefficient matrix $\mathbf{A}$ is

$$\Delta = \det(\mathbf{A} - s\mathbf{I}) =$$

$$s^4 + [2\mu\omega^2 + 2\gamma\omega]s^2 + [\mu^2\omega^4 + 2\mu\gamma\omega^3 + \gamma\omega^2 - k^2] + [\mu\omega^2 + \gamma\omega][k(G_1 + G_2)]e^{-\omega\tau} + k^2G_1G_2e^{-2\omega\tau}. \quad (4.20)$$

4.9 Alternative Formulation of Self-Delay Coupled Cantilever System and Its Results

The self-coupled version of the two cantilever system with the same physical constants as (4.6) yields the following stability plots, after computing the determinant:

$$\det \begin{bmatrix} s & -1 & 0 & 0 \\ p^4 + 0.1G_1e^{-s\tau} & s + 0.005 & 0.6 & 0 \\ 0 & 0 & s & -1 \\ 0.6 & 0 & p^4 + 0.1G_2e^{-s\tau} & s + 0.005 \end{bmatrix},$$

as the characteristic equation of the system. In following the same procedure as in (4.6 - 4.12), we obtain the following plots.
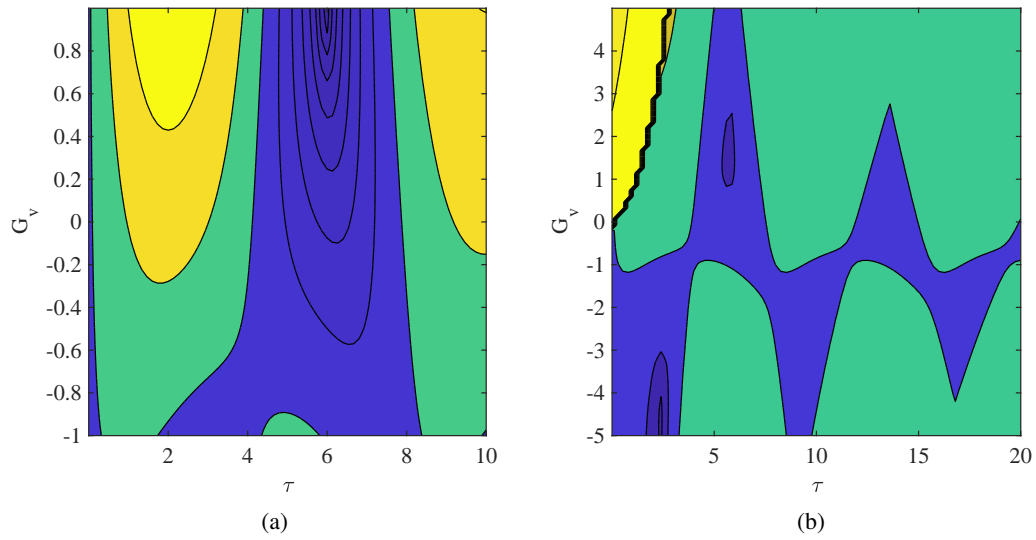
Figure 11.: (a) Self-delay coupled cantilevers, $p = 0.1$ and $G_c = 1$. Blue is stable. (b) Self-delay coupled cantilevers, $p = 0.5$ and $G_c = 1$. Blue is stable.
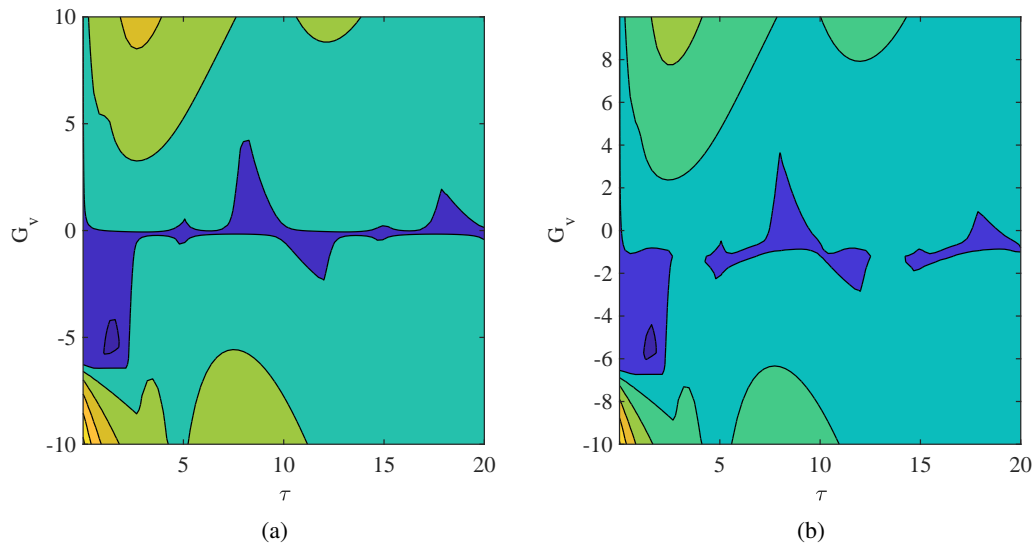
Figure 12.: Self-delay coupled cantilevers. (a) $p = 0.1$ and $G_c = 0.1$. Blue is stable. (b) $p = 1$ and $G_c = 1$. All blue regions are stable.
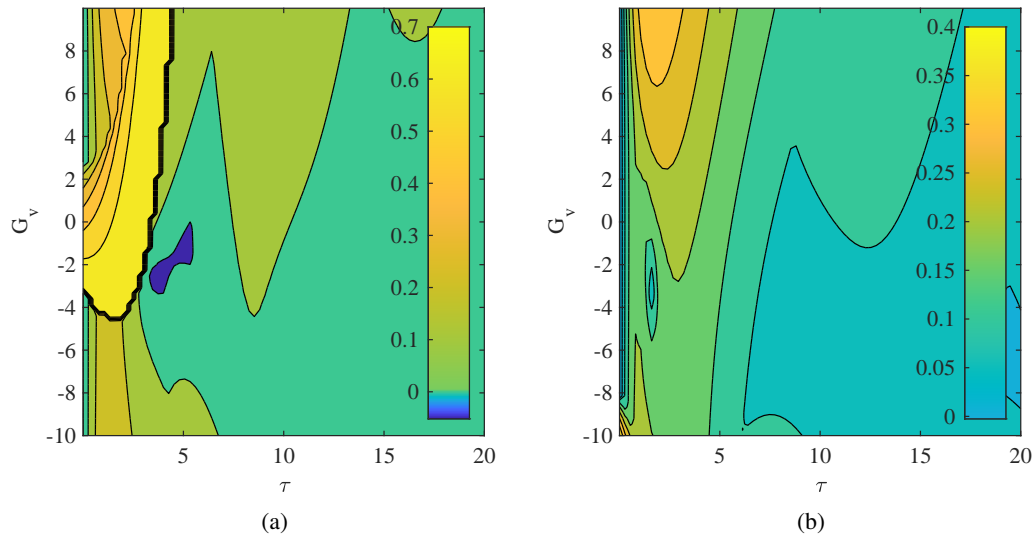
Figure 13.: (a) Self-delay coupled cantilevers, $p = 0.5$ and $G_c = 10$. Blue is stable. (b) Self-delay coupled cantilevers, $p = 1$ and $G_c = 10$. No stability found.
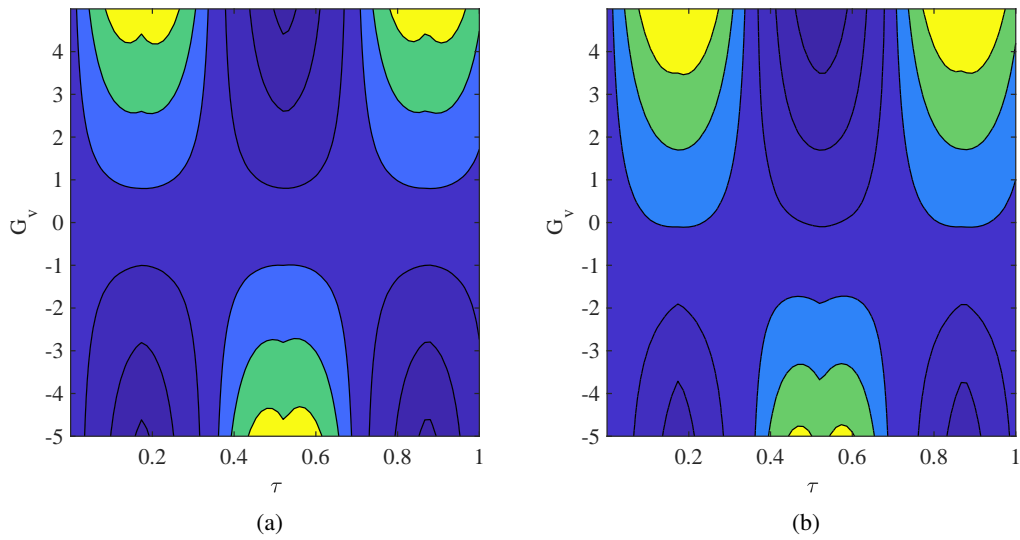
Figure 14.: (a), (b) Self-delay coupled cantilevers. Dark blue is stable. (a) $p = 3$ and $G_c = 0.1$. (b) $p = 3$ and $G_c = 1$.
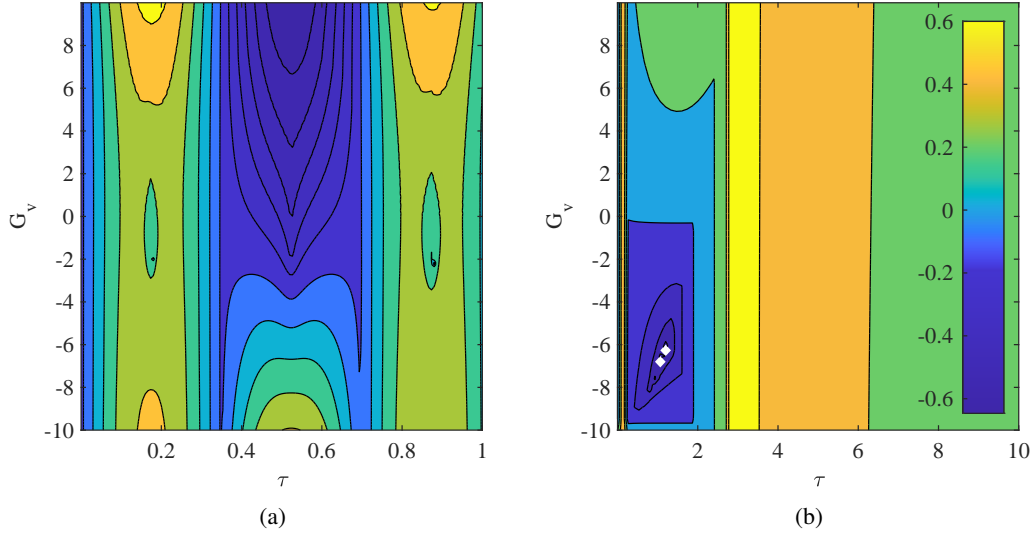
Figure 15.: (a) Self-delay coupled cantilevers, $p = 3$ and $G_c = 10$. Dark blue region is stable. (b) Self-delay coupled cantilevers, $p = 1$ and $G_c = 100$. Dark blue is stable.

4.10 Conclusion for Self-Delay Coupled Cantilevers

Modeling of the self-coupled beam case predicts that in general, as delay time increases for small or moderate delay the system tends to alternate between stability and instability, at least for smaller ranges of delay time 0 through τ, similarly to the modeling results of the single cantilever beam with delay in [20]. The alternation is roughly periodic for the parameter regions considered. The regions of stability tend to be somewhat connected, while in most of the cases we plotted for this beam setup the regions of instability appear isolated. As magnitude of gain increases, the regions of stability seem to shrink until each region terminates after reaching sufficiently large magnitude of gain levels. Although it rarely happens, some parameter and plot window choices near the origin of both axes in the gain-delay plane can and do result in no stability regions being present, according to our model. The stability regions in our self-coupled beam plots appear to be much more complex in shape than the ones obtained via either the single beam model in [20] or the coupled harmonic oscillator model in [15]. Furthermore, using different parameters in the equation setup for the self-coupled cantilever can result in drastically different shapes of the stable

regions. Possible future research topics in this area could be introducing more coupled cantilevers into the plant model and/or having different types of coupling than the types we used in this paper.

A.1 Additional Verification
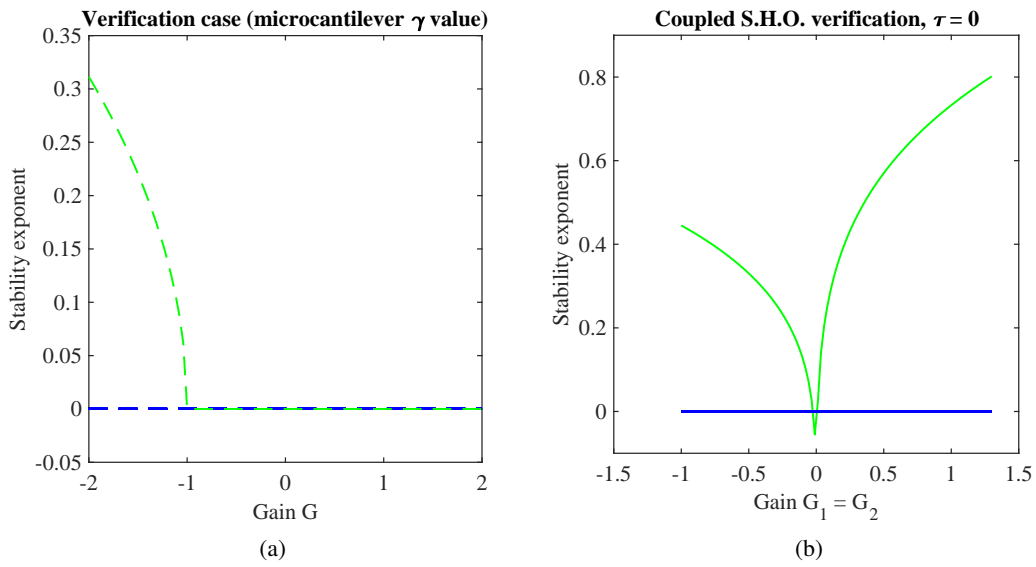
Figure 16.: (a) Single harmonic oscillator stability plot for verification for $\tau = 0$ constant. Stability holds for all gain $G \geq -1$. (b) Coupled simple harmonic oscillator stability plot for delay time zero, for verification. The damping constant here is taken to be orders of magnitude higher than typical microcantilever values, i.e. we take $\gamma = 0.5$. The system is unstable for any nontrivial gain G. We modeled as with the system in Fig. 3, with both gains G_i equal to each other.
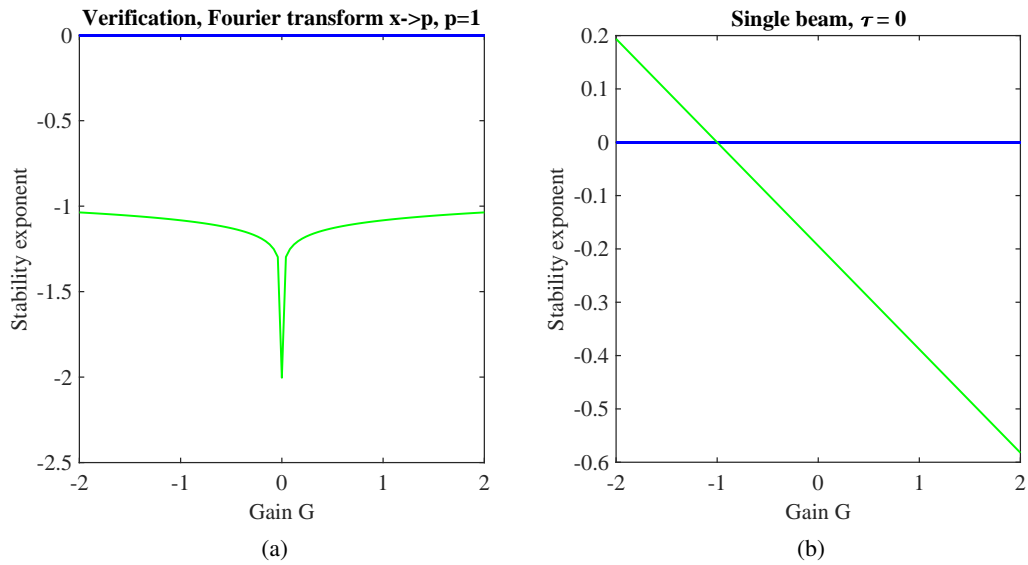
Figure 17.: (a) Single beam with delay $\tau \to \infty$ stability plot for verification. Note that the entire graphed region is stable. (b) Single beam with delay τ stability plot for verification with $\tau = 0$, $\gamma = 0.5$, and $p = 0.1$.
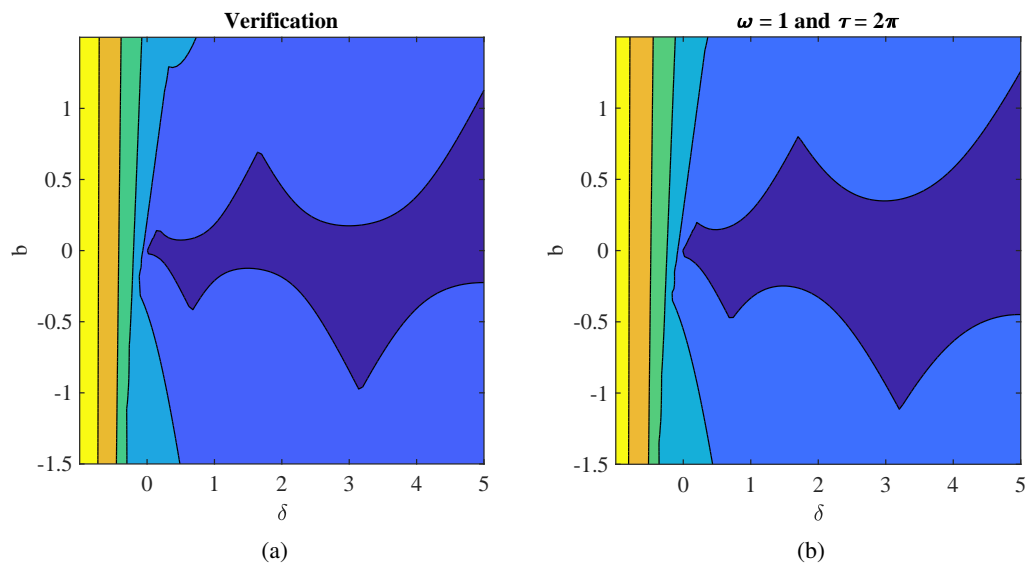
Figure 18.: Verification of plots from [17]. The darkest blue area is stable. (a) Fig 5(b) from reference. (b) Fig 5(c) from reference.

A.2 Coupled Harmonic Oscillators and Cross-Coupled Beams

(a)

(b)
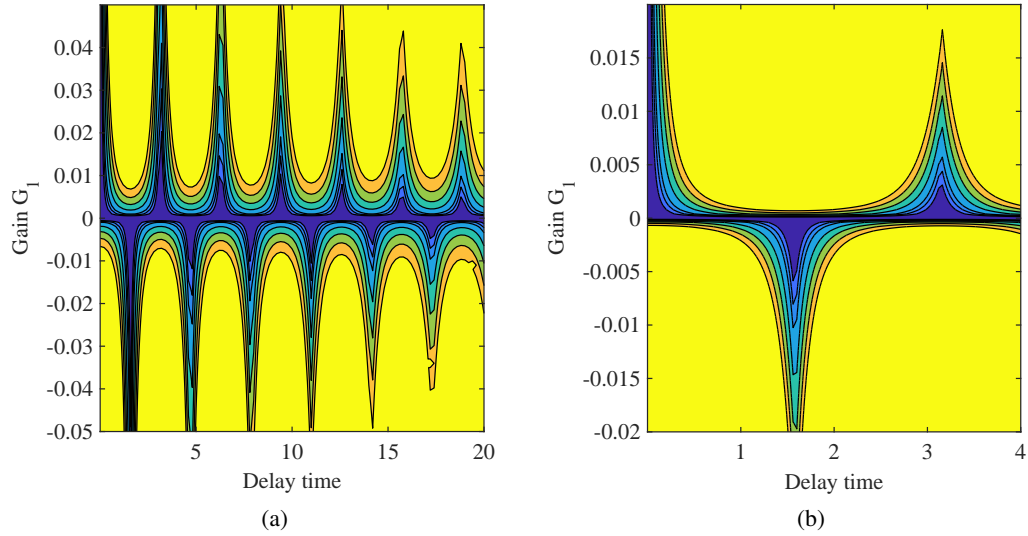
Figure 19.: (a) Stability exponent map of coupled harmonic oscillators for $G_2 = 0.1$. The darkest blue area is stable and all other colors are unstable. (b) Stability exponent map of coupled harmonic oscillators for $G_2 = 1.0$. Darkest blue area is stable, all other colors are unstable.

(a)

(b)
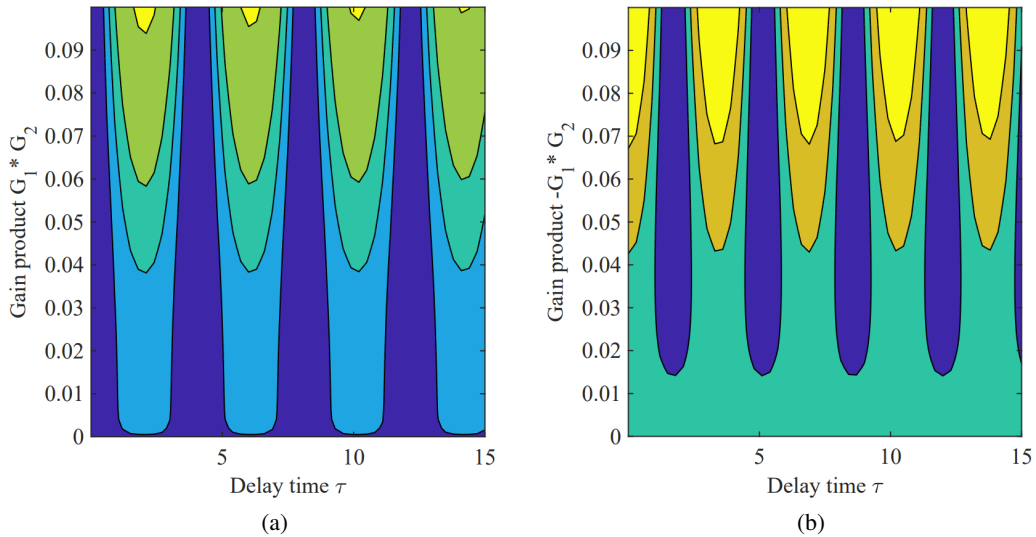
Figure 20.: (a) Cross-coupled cantilevers. Darkest blue is stable, p=0.1. (b) Cross-coupled cantilevers. Dark blue is stable, p=0.7.
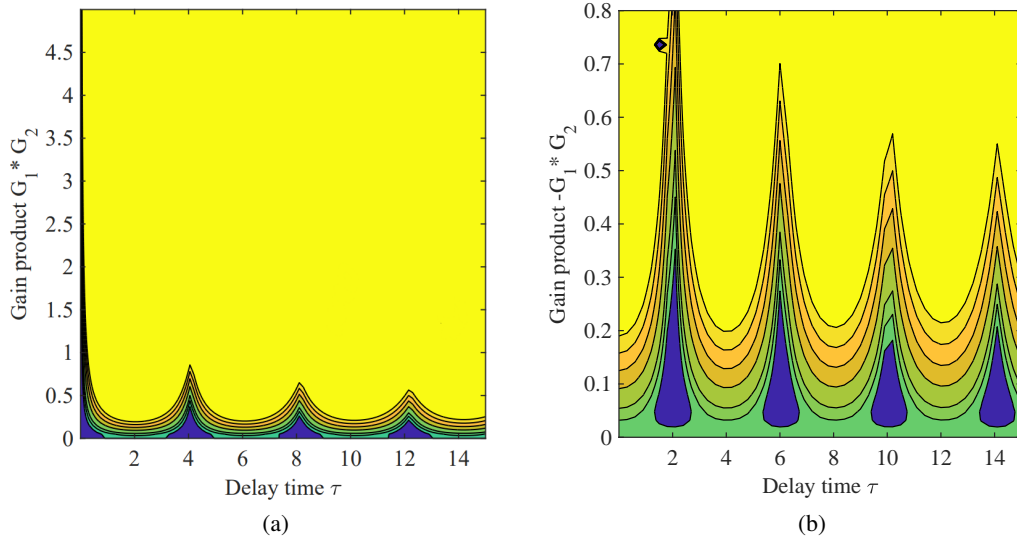
Figure 21.: (a) Cross-coupled cantilevers. Darkest blue is stable, p=0.1.   (b) Cross-coupled cantilevers. Darkest blue is stable, p=0.3.
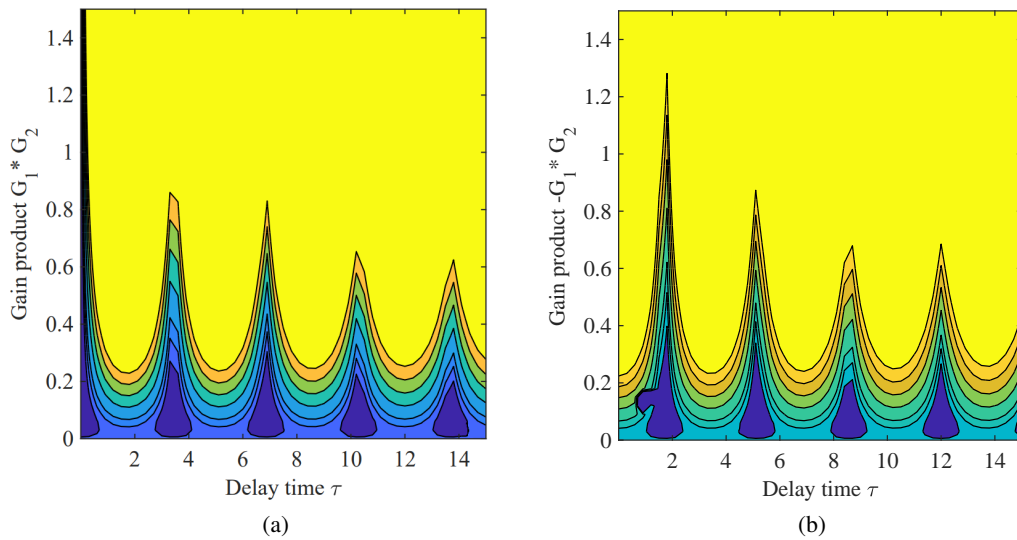
Figure 22.: Darkest blue is stable. (a) Cross-coupled cantilevers, positive product of gains. p=0.7. (b) Cross-coupled cantilevers, negative product of gains. p=0.7.
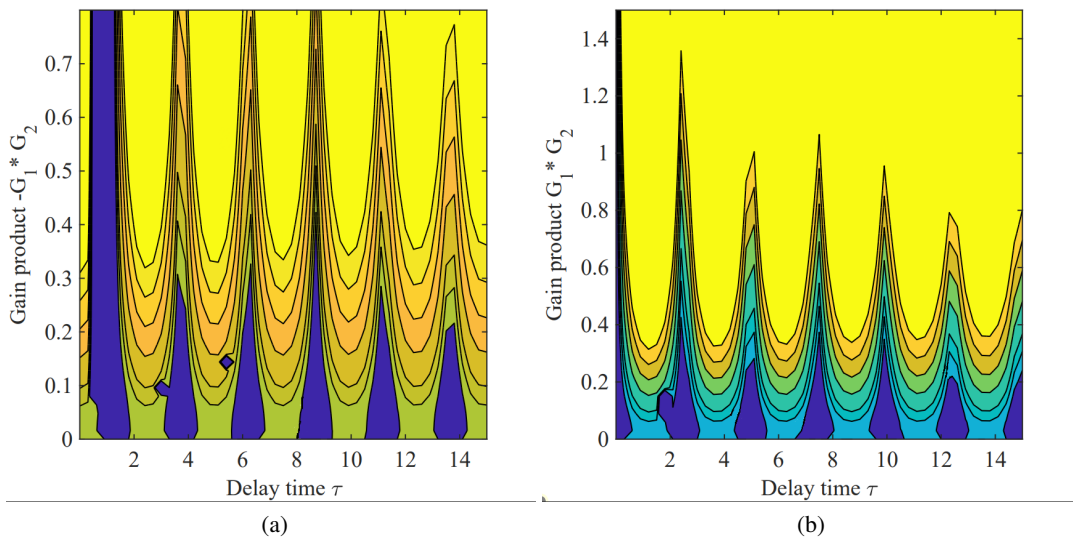
Figure 23.: Cross-coupled cantilevers, p=1.0. Dark blue is stable. (a) With negative product of gains. (b) With positive product of gains.
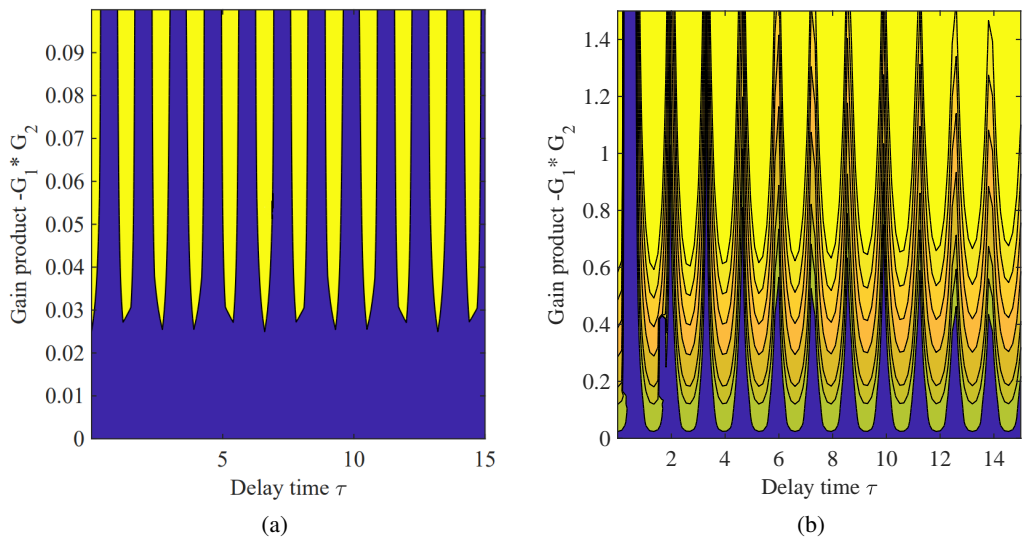

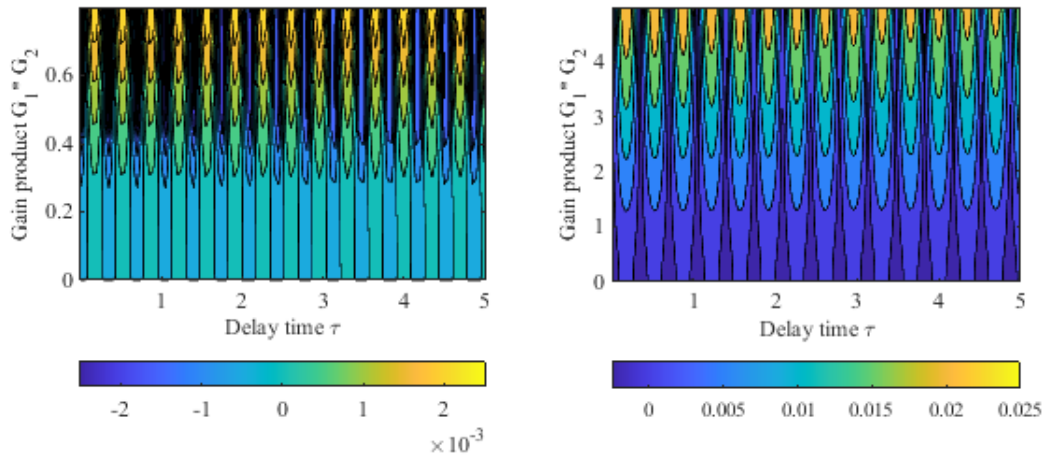Figure 24.: Cross-coupled cantilevers, p=1.5. Dark blue is stable.
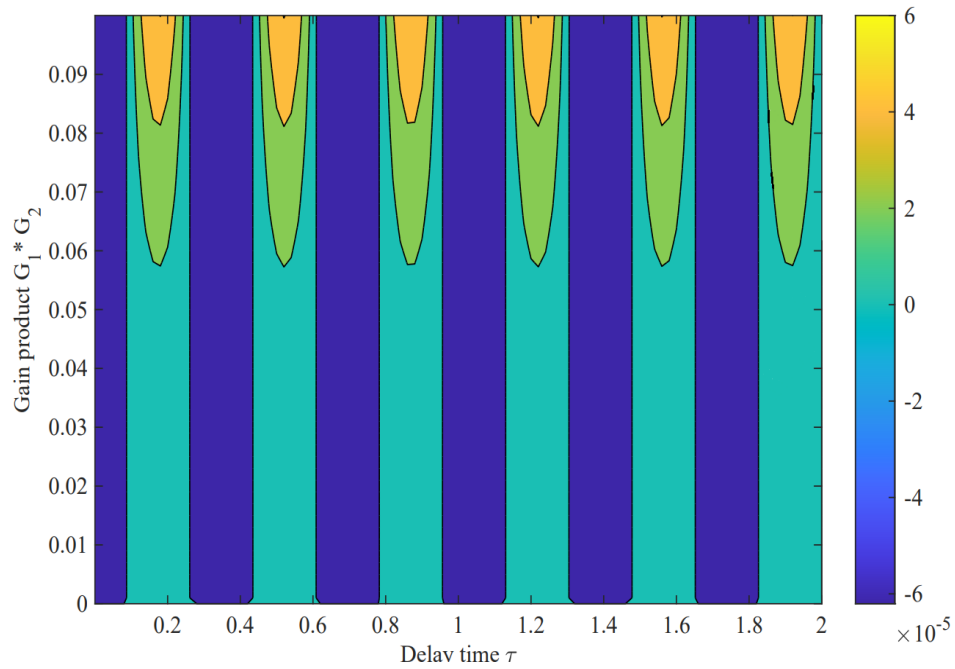
Figure 25.: Cross-coupled cantilevers, p=3.0. Darkest blue is stable.

(a)

(b)

Figure 26.: (a) Cross-coupled cantilevers. Vertical bands of equal period regions alternate between stability and instability when moving along the horizontal τ axis. Plot is with positive gain product and p=3.0. (b) Upon plotting a wider range of the gain product in more detail, it can be seen that what appeared to be vertical strips in Figs. (10a, 26a) are in fact regions that taper off and possibly vanish as gain product increases in magnitude. Here p=3.0 and $G_1 G_2 \geq 0$.
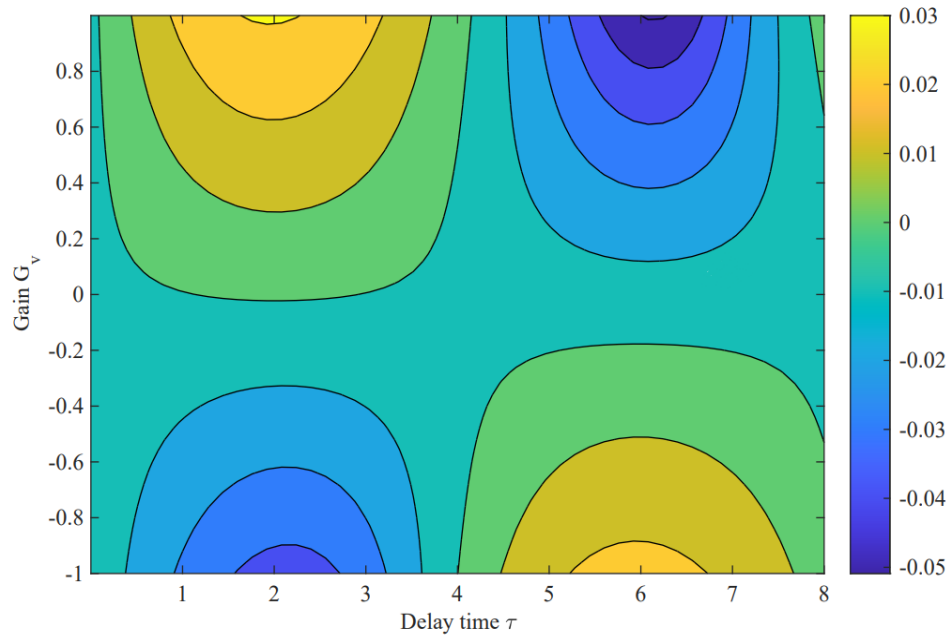
A.3 Self-Coupled Beams

Figure 27.: Self-delay coupled cantilevers, general pattern 1. $p = 0.1$ and $G_c = 0.1$.
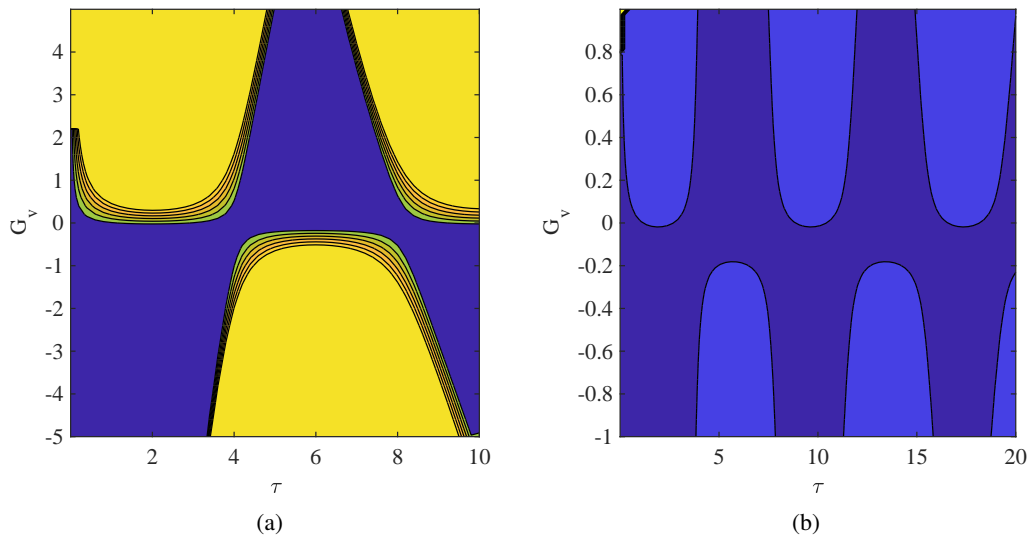

Figure 28.: Self-coupled cantilevers. (a) $p = 0.1$ and $G_c = 0.1$. Blue is stable. (b) $p = 0.5$ and $G_c = 0.1$. Dark blue is stable, blue is unstable.
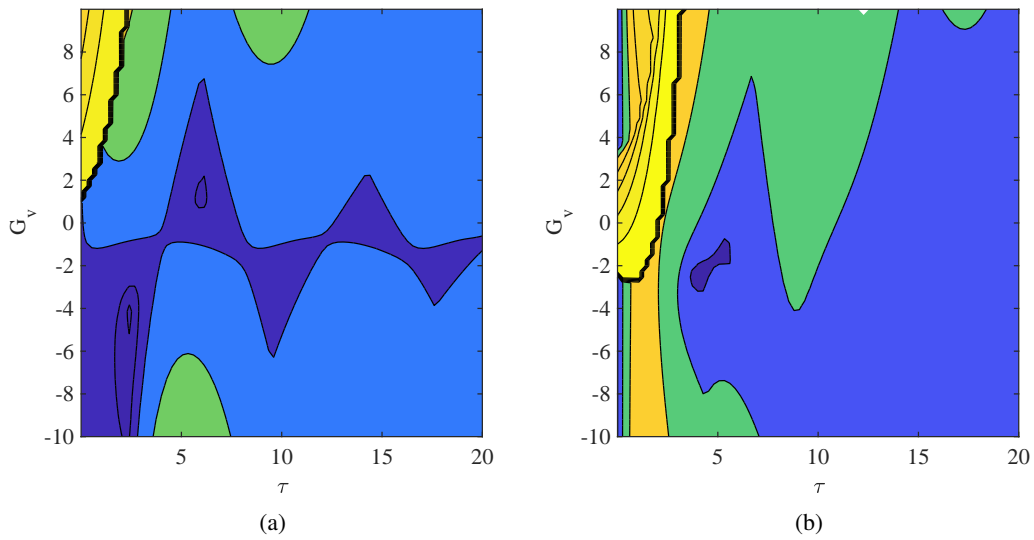
Figure 29.: (a) $p = 0.1$ and $G_c = 1$. Dark blue is stable.   (b) $p = 0.1$ and $G_c = 10$. Dark blue is stable.
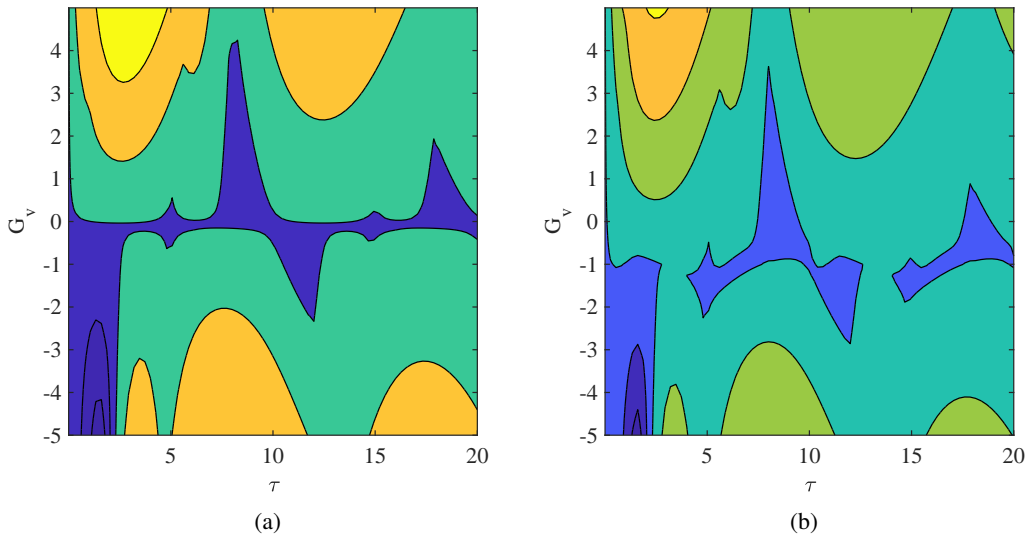

Figure 30.: Self-coupled cantilevers. All the blue regions are stable. (a) $p = 1$ and $G_c = 0.1$. (b) $p = 1$ and $G_c = 1$.
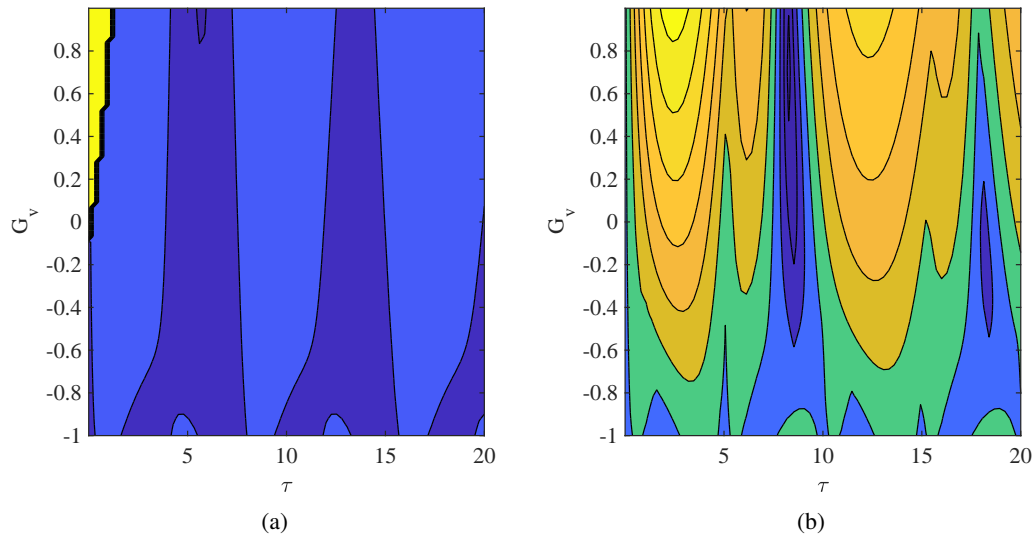
Figure 31.: (a) $p = 0.5$ and $G_c = 1$. Dark blue is stable. (b) $p = 1$ and $G_c = 1$ (Fig. 30b zoomed in). All blue regions are stable.
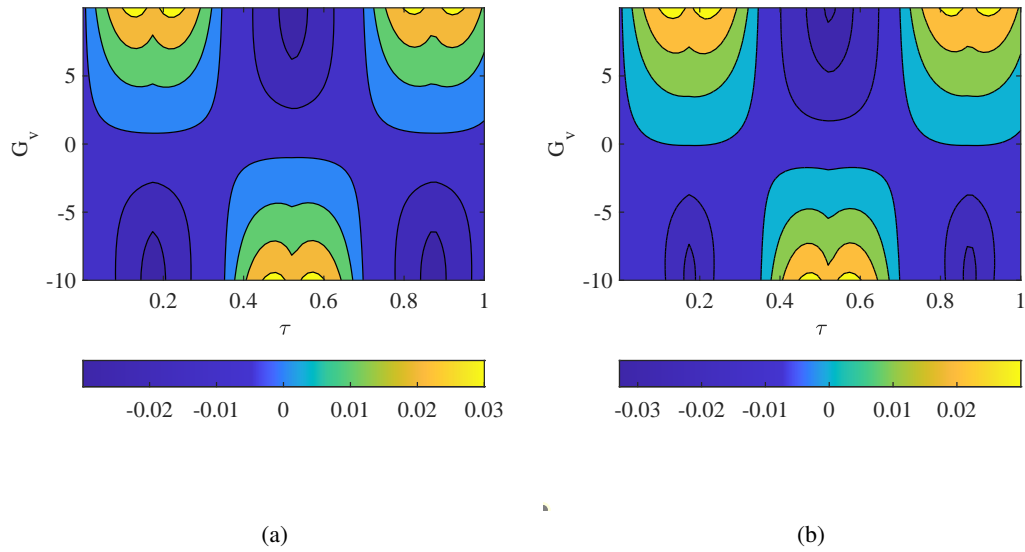

Figure 32.: Self-coupled cantilevers. Dark blue is stable. Contour lines of (a) and (b) are of different magnitude. (a) $p = 3$ and $G_c = 0.1$. (b) $p = 3$ and $G_c = 1$.
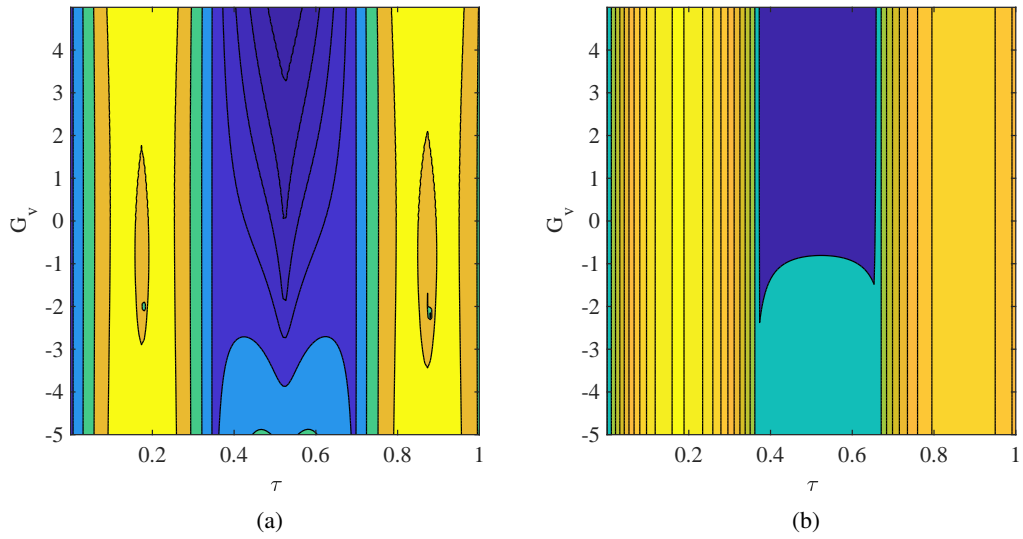
Figure 33.: (a) $p = 3$ and $G_c = 10$. Dark blue is stable. (b) $p = 3$ and $G_c = 100$. Dark blue is stable.
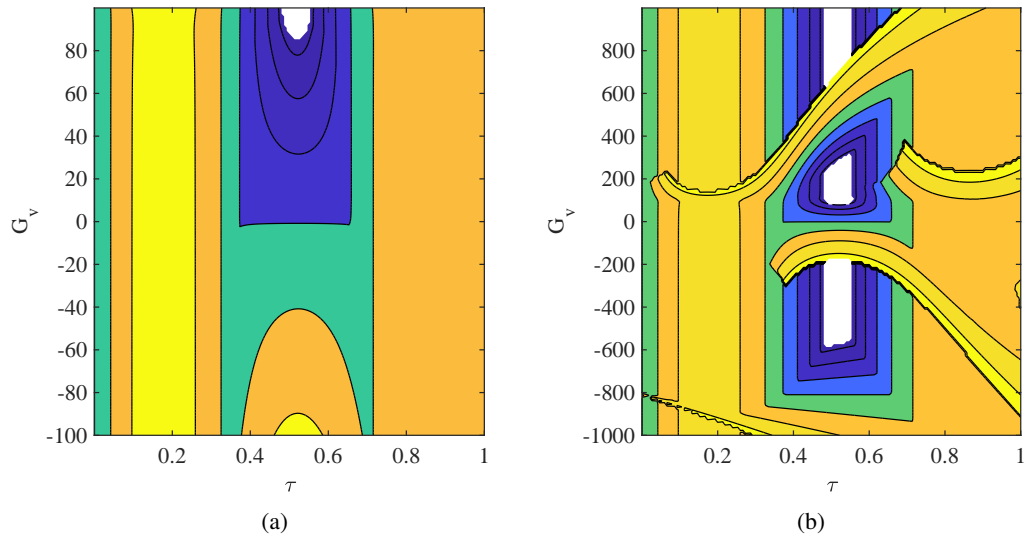

Figure 34.: (a),(b) Self-coupled cantilevers. $p = 3$ and $G_c = 100$. Blue and white are all stable.

References

[1] O. Arino, M. L. Hbid, and E. Ait Dads. Delay Differential Equations and Applications. 2006.

[2] Farshid Asl and A. Galip Ulsoy. "Analysis of a System of Linear Delay Differential Equations". In: Journal of Dynamic Systems, Measurement, and Control 125.2 (June 2003), pp. 215–223. 10.1115/1.1568121. https://doi.org/10.1115/1.1568121.

[3] L. K. Barker. "Mikhailov Stability Criterion for Time-Delayed Systems". In: United States. National Aeronautics and Space Administration. NASA Technical Reports Server : NTRS. [Washington, D.C.] :[U.S. National Aeronautics and Space Administration]. (Jan. 1979). https://ntrs.nasa.gov/api/citations/19790006688/downloads/19790006688.pdf.

[4] Alfredo Bellen and Mario Zennaro. Numerical Methods for Delay Differential Equations. 2003. https://doi.org/10.1093/acprof:oso/9780198506546.001.0001.

[5] Dimitri Breda, Stefano Maset, and Rossana Vermiglio. Stability of Linear Delay Differential Equations, A Numerical Approach with MATLAB. 2015. 10.1007/978-1-4939-2107-2. https://doi.org/10.1007/978-1-4939-2107-2.

[6] E. A. Cardwell. "Stability of Linear and Nonlinear Delay-Differential Systems". In: Student theses: Doctoral Thesis: Ph.D (1995). https://researchportal.bath.ac.uk/en/studentTheses/stability-of-linear-and-nonlinear-delay-differential-systems.

[7] Rudy Cepeda-Gomez and Wim Michiels. "Some Special Cases in the Stability Analysis of Multi-dimensional Time-delay Systems Using the Matrix Lambert W function". In: Automatica 53 (Feb. 2015), pp. 339–345. 10.1016/j.automatica.2015.01.016. https://doi.org/10.1016/j.automatica.2015.01.016.

[8] Y. Chu. "Synthesis of Feedback Control System by Phase-Angle Loci". In: Transactions of the American Institute of Electrical Engineers, Part II: Applications and Industry 71.5 (Nov. 1952), pp. 330–339. 10.1109/TAI.1952.6371287. https://doi.org/10.1109/TAI.1952.6371287.

[9] R. M. Corless et al. "On The Lambert W Function". In: Advances in Computational Mathematics 5 (Dec. 1996), pp. 329–359. https://link.springer.com/article/10.1007/BF02124750.

[10] J. H. Davis. Differential Equations with Maple: An Interactive Approach. 2001. 10.1007/978-1-4612-1376-5˙8. https://doi.org/10.1007/978-1-4612-1376-5˙8.

[11] Serbun Deger and Yasar Bolat. "Stability Conditions of a Class of Linear Retarded Differential Systems". In: International Journal of Analysis and Applications 16.4 (2018), pp. 454–461. 10.28924/2291-8639. https://doi.org/10.28924/2291-8639.

[12] Odo Diekmann et al. Delay Equations: Functional-, Complex-, and Nonlinear Analysis. 1995. 10.1016/j.automatica.2015.01.016. https://doi.org/10.1016/j.automatica.2015.01.016.

[13] Yulia Emilianova, Valeriy Emilyanov, and Nikita Ryskin. "Synchronization of Two Coupled Multimode Oscillators with Time-Delayed Feedback". In: Communications in Nonlinear Science and Numerical Simulation 19.10 (2014), pp. 3778–3791. 10.1016/j.cnsns.2014.03.031. https://doi.org/10.1016/j.cnsns.2014.03.031.

[14] Keqin Gu, Vladimir L. Kharitonov, and Jie Chen. Stability of Time-Delay Systems. 2012.

[15] Saurabh Keni. "Stability Analysis and Decentralized Control of Coupled Oscillators with Feedback Delays". In: All Theses (July 2008). https://tigerprints.clemson.edu/all˙theses/416.

[16] Hans Petter Langtangen and Geir K. Pedersen. Scaling of Differential Equations. Jan. 2016.

[17] B. P. Mann and B. R. Patel. "Stability of Delay Equations Written as State Space Models". In: Journal of Vibration and Control 16.7–8 (2010), pp. 1067–1085. 10.1177/1077546309341111. https://doi.org/10.1177/1077546309341111.

[18] W. Michiels and Tomáš Vyhlídal. "An Eigenvalue Based Approach for the Stabilization of Linear Time-Delay Systems of Neutral Type". In: Automatica 41.6 (2005), pp. 991–998.

[19] G. Muralidharan et al. "Analysis of Amplification of Thermal Vibrations of a Microcantilever". In: Journal of Applied Physics 89 (Mar. 2001), pp. 4587–4591. 10.1063/1.1357779. https://doi.org/10.1063/1.1357779.

[20] A. Passian, G. Muralidharan, and Sherwin Kouchekian. "Dynamics of Self-Driven Microcantilevers". In: Journal of Applied Physics 91 (Mar. 2002), pp. 4693–4700. 10.1063/1.1452771. https://doi.org/10.1063/1.1452771.

[21] A. Patil. "Routh-Hurwitz Criterion for Stability: An Overview and Its Implementation on Characteristic Equation Vectors Using MATLAB". In: Emerging Technologies in Data Mining and Information Security. Advances in Intelligent Systems and Computing 1286 (June 2021). 10.1007/978-981-15-9927-9˙32. https://doi.org/10.1007/978-981-15-9927-9˙32.

[22] Thomas D. Rossing and Neville Fletcher. Principles of Vibration and Sound. 2004. https://doi-org.ezproxy.lib.usf.edu/10.1007/978-1-4757-3822-3.

[23] Tomáš Vyhlídal and Pavel Zítek. "Mapping Based Algorithm for Large-Scale Computation of Quasi-Polynomial Zeros". In: IEEE Transactions on Automatic Control 54.1 (2009), pp. 171–177.

[24] Tomáš Vyhlídal and Pavel Zítek. "QPmR - Quasi-Polynomial Root-Finder: Algorithm Update and Examples". In: Delay Systems: From Theory to Numerics and Applications, Advances in Delays and Dynamics 1 (Jan. 2014). http://link.aip.org/link/?RSI/62/1/1.

[25] Tomáš Vyhlídal and Pavel Zítek. "Quasipolynomial Mapping Based Rootfinder for Analysis of Time Delay Systems". In: Time Delay Systems 2003 – A Proceedings volume from the 4th IFAC workshop, Rocquencourt, France (2003), pp. 227–232.

[26] Yong Xu et al. "Stability Analysis of an Ensemble of Simple Harmonic Oscillators". In: www.researchgate.net *(preprint)* (Apr. 2020).

[27] Xueyan Yang and Xiaodi Li. "Finite-Time Stability of Linear Non-Autonomous Systems With Time-Varying Delays". In: Advances in Difference Equations 2018 101 (Mar. 2018). 10.1186/s13662-018-1557-3. https://doi.org/10.1186/s13662-018-1557-3.

[28] Sun Yi. "Time-Delay Systems: Analysis and Control Using the Lambert W Function". In: Dissertation. University of Michigan (2009). https://www.proquest.com/openview/14fc48ed633a978f82d313f11a47f15b/1?pq-origsite=gscholar&cbl=18750.

[29] Sun Yi, Patrick W. Nelson, and A. Galip Ulsoy. "Analysis of Systems of Linear Delay Differential Equations Using the Matrix Lambert Function and the Laplace Transformation". In: Automatica 5 (Jan. 2006).

[30] Sun Yi, Patrick W. Nelson, and A. Galip Ulsoy. "Controllability and Observability of Systems of Linear Delay Differential Equations via the Matrix Lambert W Function". In: 2007 American Control Conference (July 2007), pp. 5631–5636. 10.1109/ACC.2007.4282376. https://doi.org/10.1109/ACC.2007.4282376.

[31] Sun Yi, Patrick W. Nelson, and A. Galip Ulsoy. "Delay Differential Equations via the Matrix Lambert W Function and Bifurcation Analysis: Application to Machine Tool Chatter". In: Mathematical Biosciences and Engineering 4.2 (Feb. 2007), pp. 355–368. 10.3934/mbe.2007.4.355. https://doi.org/10.3934/mbe.2007.4.355.

[32] Sun Yi, Patrick W. Nelson, and A. Galip Ulsoy. "Solution of Systems of Linear Delay Differential Equations via Laplace Transformation". In: Proceedings of the 45th IEEE Conference on Decision and Control (2006), pp. 2535–2540. 10.1109/CDC.2006.377712. https://doi.org/10.1109/CDC.2006.377712.

[33] Sun Yi and A. Galip Ulsoy. "Solution of a System of Linear Delay Differential Equations Using the Matrix Lambert Function". In: Proc. 25th American Control Conference (June 2006), pp. 2433–2438. 10.1109/ACC.2006.1656585. https://doi.org/10.1109/ACC.2006.1656585.

[34] Sun Yi et al. "The Lambert W Function Approach to Time Delay Systems and the *LambertWDDE* Toolbox". In: IFAC Proceedings Volumes 45.14 (June 2012), pp. 114–119. 10.3182/20120622-3-US-4021.00008. https://doi.org/10.3182/20120622-3-US-4021.00008.

[35] Li Zhang and Gabor Stepan. "Exact Stability Chart of an Elastic Beam Subjected to Delayed Feedback". In: Journal of Sound and Vibration 367 (Apr. 2016), pp. 219–232. 10.1016/j.jsv.2016.01.002. https://doi.org/10.1016/j.jsv.2016.01.002.

[36] T. S. Zwerkina. "Approximate Solution of Differential Equation with Retarded Argument and Differential Equations with Discontinuous Right-Hand Side". In: Trudy Sem. Teor. Differential Uravnenii s Otklon. Argumemtom Univ. Druzby Narodov Patrisa Lumumby 1 (1952), pp. 76–93. 10.1109/TAI.1952.6371287. https://doi.org/10.1109/TAI.1952.6371287.